254

Dielectric Response Methods for Diagnostics of Power Transformers

Report of the TF D1.01.09

Task Force members:
S.M. Gubanski (chair), P. Boss, G. Csépes, V. Der Houhanessian, J. Filippini, P. Guuinic, U. Gäfvert, V. Karius, J. Lapworth, G. Urbani, P. Werelius, W. Zaengl.

21 RUE D'ARTOIS, F-75008 PARIS
Tel : + (0)1 53 89 12 90 Fax + 33 (0)1 53 89 12 99
http://www.cigre.org

Dielectric Response Methods for Diagnostics of Power Transformers

Report of the TF D1.01.09

Task Force members:
S.M. Gubanski (chair), P. Boss, G. Csépes, V. Der Houhanessian, J. Filippini, P. Guuinic, U. Gäfvert, V. Karius, J. Lapworth, G. Urbani, P. Werelius, W. Zaengl.

1 INTRODUCTION

The dryness and ageing state of the oil-paper insulation is a key factor in both the short and long term reliability of a power transformer since moisture has deleterious effects on dielectric integrity and insulation ageing rates. Today the water content of the cellulose of a transformer in service is determined indirectly via moisture measured from oil samples according to IEC 60422. Moisture distributes unequally between the oil and the pressboard, the greater part residing within the solid insulation [1]. Because the water concentration in the oil is highly temperature dependent, the measurement of moisture in oil is not a particularly reliable indicator of dryness in the cellulose, particularly not for lightly loaded transformers. Although in principle moisture can also be extracted from pressboard samples and measured, this approach is hampered by the impossibility of obtaining samples from critical locations. Furthermore, a significant variation in results can arise from different practices regarding sample storage and preparation.

Recent attention has been directed to methods of determining moisture content and ageing of the pressboard and paper more directly by measuring the effects of moisture on electrical properties. Rather than the traditional measurement of power frequency loss angle, measuring

various dielectric response parameters, which characterise some known polarisation phenomena, has been in focus. The three foremost techniques are:

- Return voltage measurements (RVM), sometimes also called recovery voltage,
- Dielectric spectroscopy in time domain, i.e. measurements of polarisation and depolarisation currents (PDC),
- Dielectric frequency domain spectroscopy (FDS), i.e. measurements of electric capacitance C and loss factor $tg\delta$ in dependency of frequency.

Until recently the RVM technique has by far been the most frequently used method. However, there has been much controversy surrounding the technique [2, 3], which has been criticised on various grounds:

- moisture determinations, as derived by the evaluation method used [4, 5], are often much higher than obtained by other methods,
- the recommended interpretation scheme is too simplistic,
- the technique does not take into account dependencies on geometry and oil properties.

On the other hand there had not been much knowledge available on how to interpret the results of the PDC and FDS measurements. The work in this direction has been in progress for a few recent years and more advanced tools are available today [6, 7]. The possibilities of modelling the transformer insulation properties as well as of comparing the data obtained by means of the three techniques have been developed.

As a result CIGRE Working Group12.18.TF 4 reviewed the opinions of users of polarisation techniques and concluded that although such techniques showed promise, more work was required to validate the techniques and improve the interpretation of results. Subsequently Task Force 15.01.09 was set up in 1999 to compare the three main techniques. Initial work has concentrated on measurements with all the techniques used on an insulation model. The model was designed specifically to investigate the influence of insulation geometry on dielectric responses. Comparisons using a mathematical model of polarisation behaviour, was also done. Furthermore, the influences of the thermodynamic moisture equilibrium between paper and oil as well as the oil conductivity were tested with this model. In parallel, number of activities were undertaken in UK, Switzerland and Sweden, which included measurements with the different techniques on selected power transformers under field conditions.

This report summarises the work performed by TF 15.01.09 and presents conclusions regarding the state of the knowledge on the applicability of the techniques. A general background for understanding the polarisation phenomena in electrical insulation is provided first. The relations derived are essential for understanding and processing the data obtained from dielectric measurements. It is followed by a description of the theoretical principles for the polarisation measurements and, in particular, for the three techniques used. Special emphasis is put to the description on how to interpret and model the results obtained. Then the model experiments are described and analysed. Finally, the study cases from UK and Sweden are mentioned. List of relevant references and other related literature is provided at the end of the report as well.

2 BACKGROUND

2.1 Dielectric response in time domain

In insulating media, also called dielectrics, which are in general isotropic and homogeneous, the vectors of dielectric displacement, $\boldsymbol{D}$, electric field, $\boldsymbol{E}$, and polarisation, $\boldsymbol{P}$, are of equal direction and interrelated by

$$\boldsymbol{D} = \varepsilon_0 \boldsymbol{E} + \boldsymbol{P} \qquad (2.1)$$

The physical constant, $\varepsilon_0 = 8.854 \cdot 10^{-12}$ As/Vm, is the permittivity of vacuum, the dimension and magnitude of which converts the dimension of the electric field (V/m) into the dimension of the dielectric displacement (As/m^2). Moreover, the relation between the dielectric displacement, $\boldsymbol{D}$, and the applied field, $\boldsymbol{E}$, is often and in general linear. The relation can be then expressed with a simple proportionality factor, ε

$$\boldsymbol{D} = \varepsilon\varepsilon_0 \boldsymbol{E} \qquad (2.2)$$

The factor ε is called relative permittivity and it describes the dielectric properties of the medium. It therefore appears that the polarisation, $\boldsymbol{P}$, must also be proportional to the field, $\boldsymbol{E}$

$$\boldsymbol{P} = \chi\varepsilon_0 \boldsymbol{E} \equiv \varepsilon_0 (\varepsilon - 1)\boldsymbol{E} \qquad (2.3)$$

This equation assumes linearity of the system. The quantity χ is called the dielectric susceptibility of the medium.

All the equations presented above describe the vectorial conditions. However, the polarisation in materials is a time dependent, and therefore also a frequency dependent, phenomenon and can be caused by several mechanisms [8]: electronic, ionic (molecular), dipolar (orientation), and interfacial. Furthermore, hopping of charge carriers between localised sites also creates polarisation [9]. The first two types of polarisation are extremely fast. For this reason, depending on the time scale used, the fast polarisation mechanisms can together be considered as instantaneous, $\boldsymbol{P}(\boldsymbol{t} = \boldsymbol{t}_0) = \boldsymbol{P}_\infty$. Moreover, the polarisation has to saturate, i.e. it must be finite at longer times, $\boldsymbol{P}(\boldsymbol{t} \to \infty) = \boldsymbol{P}_s$. Figure 1 shows the polarisation for a medium when a step-like constant electric field, $\boldsymbol{E} = \text{const}$, is applied at $\boldsymbol{t}_0$ (note that $\boldsymbol{t}_0$ can vary freely over the whole time scale). The time dependent polarisation is then

$$\boldsymbol{P}(\boldsymbol{t}) = \boldsymbol{P}_\infty + (\boldsymbol{P}_s - \boldsymbol{P}_\infty)\boldsymbol{g}(\boldsymbol{t} - \boldsymbol{t}_0) \qquad (2.4)$$

where $\boldsymbol{g}(\boldsymbol{t})$ is a monotonically positive increasing function of time

$$\boldsymbol{g}(\boldsymbol{t}) \geq 0, \qquad \frac{\partial \boldsymbol{g}(\boldsymbol{t})}{\partial \boldsymbol{t}} \geq 0, \qquad \text{for all} \qquad 0 < \boldsymbol{t} < \infty$$

and

$$g(t) = \begin{cases} 0 & \text{if} \quad t \le 0 \\ 1 & \text{if} \quad t \to \infty \end{cases}$$

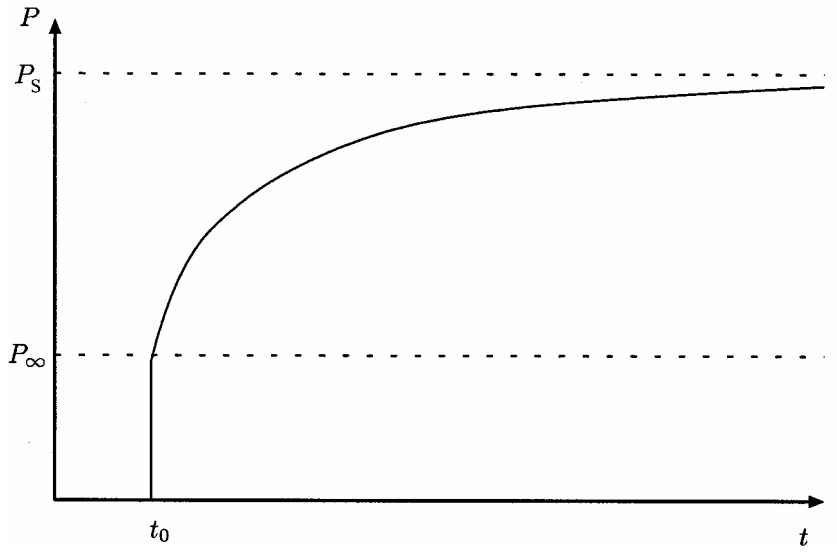

Figure 1 Time variation of polarisation when a constant electric field is applied at $t = t_0$.

For an applied step-like constant electric field, and introducing equation (2.3), the polarisation in this case becomes

$$\boldsymbol{P}(t) = \varepsilon_0\left[(\varepsilon_\infty - 1) + (\varepsilon_s - \varepsilon_\infty)g(t - t_0)\right]\boldsymbol{E} \qquad \textbf{(2.5)}$$

Here, the two values , ε_s and ε_∞, are the "static" (i.e. for a selected frequency static) and "instantaneous" (high frequency) relative permittivities.

Starting from this relation and when applying the superposition principle, one can show that for linear, homogeneous and isotropic dielectrics, when now a time varying electric field, $\boldsymbol{E}(t)$, is considered, the polarisation can be defined as

$$\boldsymbol{P}(t) = \varepsilon_0(\varepsilon_\infty - 1)\boldsymbol{E}(t) + \varepsilon_0 \int_{-\infty}^{t} f(t - t_0)\boldsymbol{E}(t_0)\,dt_0 \qquad \textbf{(2.6)}$$

where $f(t)$ describes so called response function of the dielectric, and it is equal to

$$f(t) = -(\varepsilon_s - \varepsilon_\infty)\frac{\partial g(t)}{\partial t} \qquad \textbf{(2.7)}$$

$f(t)$ is a monotonically decreasing function. The dielectric displacement $\boldsymbol{D}(t)$ becomes then

$$\boldsymbol{D}(t) = \varepsilon_0\varepsilon_\infty \boldsymbol{E}(t) + \varepsilon_0 \int_{-\infty}^{t} f(t - t_0)\boldsymbol{E}(t_0)\,dt_0 \qquad \textbf{(2.8)}$$

The first part of this equation represents the fast (instantaneous) polarisation processes whereas the second part represents the slow (delayed) ones.

If a given electric field $\boldsymbol{E}(\boldsymbol{t})$ is suddenly applied across a dielectric material, both free and bonded charges it contains will give rise to a current flow. The movement of the free charges represents materials volume resistivity, whereas the bonded charges represent the dielectric displacement being a sum of the vacuum displacement current and polarisation current. The total current density is given as

$$\boldsymbol{j}(\boldsymbol{t}) = \sigma_{\boldsymbol{dc}}\boldsymbol{E}(\boldsymbol{t}) + \frac{\partial \boldsymbol{D}(\boldsymbol{t})}{\partial \boldsymbol{t}} = \sigma_{\boldsymbol{dc}}\boldsymbol{E}(\boldsymbol{t}) + \varepsilon_0 \frac{\partial \boldsymbol{E}(\boldsymbol{t})}{\partial \boldsymbol{t}} + \frac{\partial \boldsymbol{P}(\boldsymbol{t})}{\partial \boldsymbol{t}} = \sigma_{\boldsymbol{dc}}\boldsymbol{E}(\boldsymbol{t}) + \varepsilon_0\left[\varepsilon_\infty \delta(\boldsymbol{t}) + \boldsymbol{f}(\boldsymbol{t})\right]\boldsymbol{E}(\boldsymbol{t}) \quad \textbf{(2.9)}$$

The two asymptotic parts of the current, $\boldsymbol{j}(\boldsymbol{t})$, are the instantaneous current density due to the capacitive component, $\varepsilon_0\varepsilon_\infty\delta(\boldsymbol{t})$ (where $\delta(\boldsymbol{t})$ means the delta function), and the dc conduction current density due to the conductivity, $\sigma_{\boldsymbol{dc}}$, of the material, respectively. The current density due to the material polarisation is given by the response function, $\boldsymbol{f}(\boldsymbol{t})$. It is therefore seen from the equation above that the conductivity $\sigma_{\boldsymbol{dc}}$, the instantaneous (high frequency) component of the relative permittivity, ε_∞, and the dielectric response function, $\boldsymbol{f}(\boldsymbol{t})$, characterise the behaviour of the dielectric material in time domain. It is also worth of notifying that current measurements in time domain can directly lead to estimation or quantification of $\sigma_{\boldsymbol{dc}}$ and $\boldsymbol{f}(\boldsymbol{t})$.

2.2 Dielectric response in frequency domain

If we now consider the properties of materials in electric fields that have an alternating time dependence that can be described with one frequency, $\widehat{\boldsymbol{E}} = \boldsymbol{E_m}\boldsymbol{e}^{\boldsymbol{iwt}}$, the complex dielectric displacement becomes

$$\widehat{\boldsymbol{D}}(\boldsymbol{t}) = \varepsilon_0\varepsilon_\infty \boldsymbol{E_m}\boldsymbol{e}^{\boldsymbol{i\omega t}} + \varepsilon_0 \int_{-\infty}^{\boldsymbol{t}} \boldsymbol{f}(\boldsymbol{t}-\boldsymbol{t}_0)\boldsymbol{E_m}\boldsymbol{e}^{\boldsymbol{i\omega t_0}}\boldsymbol{dt}_0 \quad \textbf{(2.10)}$$

and after some simple transformations it becomes

$$\widehat{\boldsymbol{D}}(\boldsymbol{t}) = \varepsilon_0\left[\varepsilon_\infty + \int_{\boldsymbol{o}}^{\infty} \boldsymbol{f}(\boldsymbol{t})\boldsymbol{e}^{-\boldsymbol{i\omega t}}\boldsymbol{dt}\right]\boldsymbol{E_m}\boldsymbol{e}^{\boldsymbol{i\omega t}} \quad \textbf{(2.11)}$$

It appears also that the Fourier transform of the response function $\boldsymbol{f}(\boldsymbol{t})$ yields the complex susceptibility, $\widehat{\chi}(\omega)$

$$\widehat{\boldsymbol{f}}(\omega) = \int_0^{\infty} \boldsymbol{f}(\boldsymbol{t})\boldsymbol{e}^{-\boldsymbol{i\omega t}}\boldsymbol{dt} = \widehat{\chi}(\omega) = \chi'(\omega) - \boldsymbol{i}\chi''(\omega) \quad \textbf{(2.12)}$$

The real and the imaginary parts of the complex dielectric susceptibility are not independent from each other since they are both generated by the same function, the response function $\boldsymbol{f}(\boldsymbol{t})$. They can respectively be seen as the cosine and the sine transforms of the response function. By carrying out the inverse cosine and sine transforms will return $\boldsymbol{f}(\boldsymbol{t})$. This is a very important property since the Fourier transform provides a direct link between measurements of dielectric properties in time and frequency domains. Moreover, the real and the imaginary parts of the complex dielectric susceptibility are also coupled with each other by so called Kramers-Kronig relations [9]

$$\chi'(\omega) = \frac{1}{\pi} \wp \int_{-\infty}^{\infty} \frac{\boldsymbol{x}\chi''(\boldsymbol{x})}{\boldsymbol{x}-\omega} \boldsymbol{dx}$$
$$\chi''(\omega) = \frac{1}{\pi} \wp \int_{-\infty}^{\infty} \frac{\chi'(\boldsymbol{x})}{\boldsymbol{x}-\omega} \boldsymbol{dx} \qquad \textbf{(2.13)}$$

where $\wp$ represents the Cauchy principle value of the integral.

The total current density $\hat{\boldsymbol{j}}(\omega)$ in a dielectric material under $\hat{\boldsymbol{E}}(\omega)$ excitation can therefore be expressed as

$$\hat{\boldsymbol{j}}(\omega) = \boldsymbol{i}\omega\varepsilon_0 \left[\underbrace{\varepsilon_\infty + \chi'(\omega)}_{\text{capacitive part}} - \boldsymbol{i} \underbrace{\left(\frac{\sigma_{\boldsymbol{dc}}}{\varepsilon_0 \omega} + \chi''(\omega) \right)}_{\text{resistive part}} \right] \hat{\boldsymbol{E}}(\omega) \qquad \textbf{(2.14)}$$

This expression shows that the current is composed of two components, one in phase with the applied field, $\hat{\boldsymbol{E}}(\omega)$ - resistive part, and one that lies 90° before the driving field – capacitive part. The part of the current in phase with the field represents the energy lost in the material. In fact, there are two different mechanisms contributing to it, one is due to dc conduction (movement of free charges), and another due to relaxation losses (reorientation of bonded charges). The part of the current which lies 90° before the driving field is associated with the capacitance of the material.

In many situations, it is more convenient to use the complex permittivity instead of the complex susceptibility. I can be defined as follows

$$\hat{\boldsymbol{j}}(\omega) = \boldsymbol{i}\omega\varepsilon_0 [\varepsilon'(\omega) - \boldsymbol{i}\varepsilon''(\omega)] \hat{\boldsymbol{E}}(\omega) \qquad \textbf{(2.15)}$$

where $\varepsilon'(\omega) = \varepsilon_\infty + \chi'(\omega)$ and $\varepsilon''(\omega) = \frac{\sigma_{\boldsymbol{dc}}}{\varepsilon_0 \omega} + \chi''(\omega)$ $\qquad \textbf{(2.16)}$

The equations presented above show that the dc conductivity, $\sigma_{\boldsymbol{dc}}$, the high frequency component of the relative permittivity, ε_∞, and the complex dielectric susceptibility, $\hat{\chi}(\omega)$, characterise the dielectric material in frequency domain, and, as in the time domain, it is

possible to make measurements that allow to find these parameters. Under the assumption that the dielectric material is linear, homogeneous and isotropic, the information obtained in either the time or frequency domain is equal. The information found in one domain can be transformed to the other. If, however, the insulation system is composed of mixtures of several linear, homogeneous and isotropic materials, the total dielectric response is not a simple superposition of the individual contributions.

2.3 Dielectric responses of materials

The dielectric response function $f(t)$ must be finite since the steady-state polarisation is finite. Each dielectric material has its own and unique function [9]. Typical examples of different dielectric responses that can be found in electric insulation materials are illustrated inFigure 2. Such simple response functions can, in general, only be found within certain time ranges of the logarithmic time scale and may change with time.

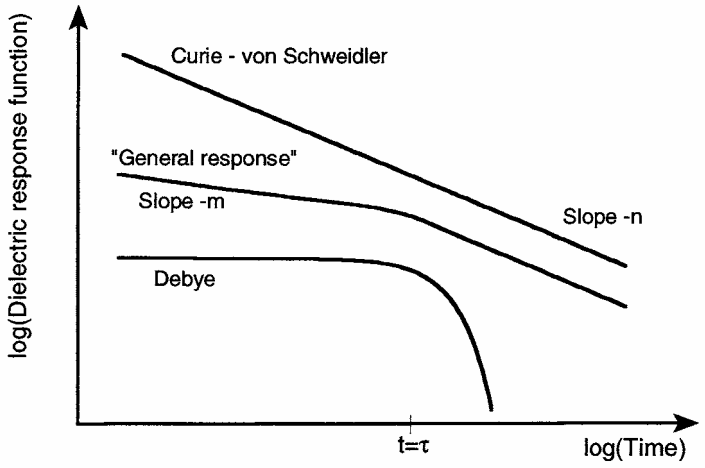

Figure 2 ***Different types of dielectric response functions, $f(t)$, in time domain. For polar liquids response functions like the Debye function are commonly found. In solid dielectrics the response functions are more of the fractional power law type, as seen in the "General response" and Curie-von Schweidler types of functions.***

The most often referenced and considered response, the classical Debye response [10], can be found in simple dielectric liquids, but is hardly seen in solid dielectric materials. Debye considered non-interacting dipoles in a viscous medium and he derived the following exponential form of the dielectric response function:

$$f(t) = \frac{\Delta\varepsilon}{\tau_D} e^{-t/\tau_D} \qquad (2.17)$$

where $\Delta\varepsilon = \varepsilon_s - \varepsilon_\infty$.

The time constant τ_D is called the Debye dielectric relaxation time, or simply the relaxation time. The complex dielectric susceptibility, $\hat{\chi}(\omega)$, after using the Fourier transform of the Debye response function is

$$\hat{\chi} = \frac{\Delta\varepsilon}{1+\boldsymbol{i}\omega\tau_{\boldsymbol{D}}} = \underbrace{\frac{\Delta\varepsilon}{1+\omega^2\tau_{\boldsymbol{D}}^2}}_{\chi'(\omega)} - \underbrace{\boldsymbol{i}\omega\tau_{\boldsymbol{D}}\frac{\Delta\varepsilon}{1+\omega^2\tau_{\boldsymbol{D}}^2}}_{\chi''(\omega)} \qquad \textbf{(2.18)}$$

In Figure 3 the frequency response of the Debye model is shown. This response can be calculated analytically from equation (2.18). Most frequently, however, the dipolar response found in materials is much wider than the Debye one and has at low frequencies the behaviour $\propto \omega^{\boldsymbol{n}}$ and at high frequencies the behaviour $\propto \omega^{\boldsymbol{m}}$. The symmetric case, $\boldsymbol{n} = \boldsymbol{m} < 1$, can be found, for example, in weakly doped ionic crystals. The asymmetric case, $\boldsymbol{n} > \boldsymbol{m}$, can be found in polymers and glasses as α- and β- relaxation peaks [9].

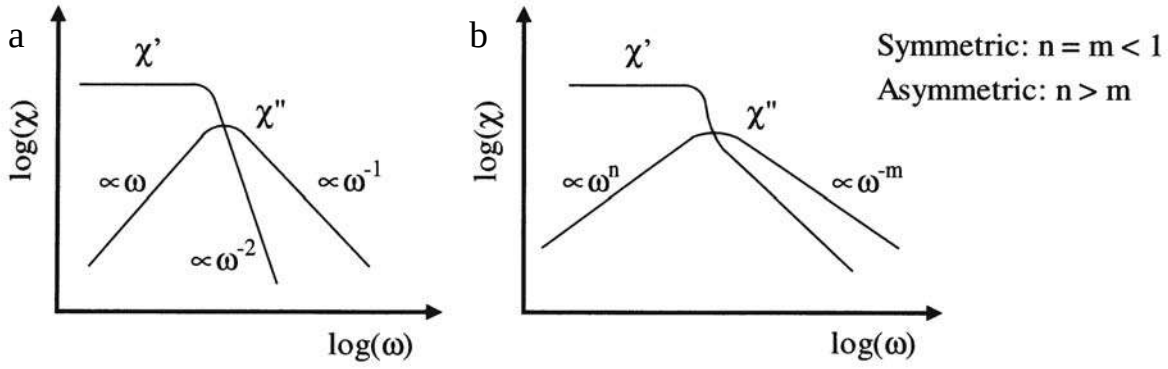

Figure 3 ***Frequency response of (a) Debye model and (b) a wider dipolar peak found in many insulating materials.***

The dielectric response functions of many solid materials (as e.g. in polyethylene or numerous other polymers) follow over a wide range of times the so-called Curie-von Schweidler model

$$\boldsymbol{f}(\boldsymbol{t}) = \boldsymbol{A}\boldsymbol{t}^{-\boldsymbol{n}} \qquad \textbf{(2.19)}$$

where $\boldsymbol{A}$ and $\boldsymbol{n}$ are constants. Both dipolar and hopping systems show this behaviour, but with different values of $\boldsymbol{n}$ in different time ranges [9]. In frequency domain there is a corresponding relation obtained via the Fourier transformation

$$\hat{\chi}(\omega) = \frac{\boldsymbol{A}\Gamma(1-\boldsymbol{n})}{(\boldsymbol{i}\omega)^{1-\boldsymbol{n}}} \qquad \textbf{(2.20)}$$

Another often seen behaviour, called the general response, represents a transition at $\boldsymbol{t} = \tau$ between different processes in a dielectric material

$$f(t) = \frac{A}{\left(t/\tau\right)^m + \left(t/\tau\right)^n} \qquad (2.21)$$

where $m > 1 > n > 0$. It is not possible to solve analytically the Fourier transform of the general response relation, but for times $t < \tau$ and times $t > \tau$ it can be approximated with the Curie-von Schweidler model.

$$t < \tau: \quad \hat{\chi}(\omega) \propto \frac{1}{(i\omega)^{1-n}} \quad \text{and} \quad t > \tau: \quad \hat{\chi}(\omega) \propto \frac{1}{(i\omega)^{1-m}} \qquad (2.22)$$

Experiments show that the general response relation fits well dipolar systems [9].

In addition to the mentioned expressions of dielectric responses, one also uses a number of modifications, which exploit combinations of the power and exponential dependencies.

Yet another behaviour in frequency domain is shown in Figure 4. The ***"a"*** type of response is mostly seen in charge carrier dominated systems, which show strong dispersion at low frequency region, called low frequency dispersion (LDF), where $\propto \omega^{-n}$, $n < 1$ [9]. The ***"b"*** response, called flat response, is present when no other mechanism is dominant. This response can be derived from Curie-von Schweidler model (equations (2.19) and (2.20)).

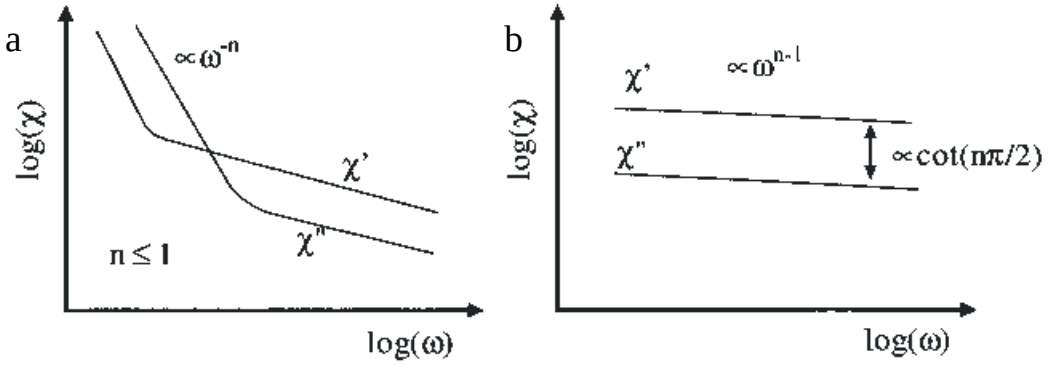

Figure 4 Frequency response of (a) hopping charges in charge carrier dominated systems and (b) flat response when no other mechanism is dominant.

Most insulating systems found in practical applications are composites or mixtures of several different dielectric materials. It is important to realise that then each material has its own dielectric response and when putting different materials together the total response will not only reflect properties of each material but also the way they are put together. This is also the case when an insulating liquid with ionic conduction is mixed with a lower conducting solid, as it is done in oil-paper insulation system. When these two media are put into contact (forming an interface), charge accumulation occurs at the interface due to the differences between their electrical properties. This kind of polarisation is called the Maxwell-Wagner [11] [12] or interfacial polarisation.

Maxwell derived the complex permittivity $\hat{\varepsilon}$ of a mixture formed by layers of two materials, which are stressed by an electric field perpendicular to the interface, as

$$\varepsilon' = \varepsilon_\infty \left(1 + \frac{\boldsymbol{K}}{1+\omega^2\tau^2} \right) \quad \text{and} \quad \varepsilon'' = \varepsilon_\infty \frac{\boldsymbol{K}}{1+\omega^2\tau^2} \qquad \textbf{(2.23)}$$

He considered that one of the layers was ideally insulating with constant permittivity ε_1. The other layer was conductive with constant permittivity ε_2 and conductivity $\sigma_{\boldsymbol{dc}2}$. The thickness ratio of the conductive layer to the thickness of the whole structure was $\boldsymbol{q}$. The constants ε_∞, $\boldsymbol{K}$, and τ in the above equations are

$$\begin{aligned} \varepsilon_\infty &= (1+2\boldsymbol{q}) \frac{\varepsilon_1 \varepsilon_2}{\boldsymbol{q}(\varepsilon_1+\varepsilon_2)+\varepsilon_2} \\ \boldsymbol{K} &= \frac{\boldsymbol{q}\varepsilon_1}{(1+\boldsymbol{q})\varepsilon_2} \\ \tau &= \frac{\boldsymbol{q}(\varepsilon_1+\varepsilon_2)+\varepsilon_2}{(1+\boldsymbol{q})\sigma_{\boldsymbol{dc}2}} \end{aligned} \qquad \textbf{(2.24)}$$

The concept of Maxwell was then extended to multi-component systems in which the constituents were characterised by own permittivity and conductivity values, for examples see [13] [14] [15] [16]. It is interesting to note, and easy to understand, that the expressions describing the permittivity of the Maxwell-Wagner polarisation are identical to those of the Debye polarisation. Identical relaxation behaviour can be modelled by means of equivalent electrical circuits of the layered structures, in which the layer electrical parameters are represented by in series- and in parallel-connected RC elements. Toady's computerised tools allow for analysing responses of quite complicated circuits. On the other hand, analyses of complex layer systems are also possible in which response functions and conductivities of constituents are provided. Both the attempts are presented in this report later.

2.4 Temperature dependence of dielectrics properties

For a quite large group of solid dielectric materials the shape of the dielectric response (spectral shape) does not change very drastically with temperature. This is at least true for temperature ranges over which the material does not change its internal structure too much (phase transitions etc.). This means that it is often possible to normalise the measurement data for different temperatures by shifting the time/frequency spectra so that they coincide into one single curve, called the "master curve" [9]. The resulting "master curve" covers a larger time/frequency range than one single temperature run, thus containing more information and also adding increased reliability in the measurement points. The "master curve" technique can be used both in the time and frequency domains. In the time domain the dielectric response function can be shifted, without changing shape, in both amplitude and time using the following expression

$$\boldsymbol{f}(\boldsymbol{t}, \boldsymbol{T}_2) = \boldsymbol{A}_y(\boldsymbol{T}_1, \boldsymbol{T}_2)\, \boldsymbol{f}\left(\boldsymbol{A}_x(\boldsymbol{T}_1, \boldsymbol{T}_2) \cdot \boldsymbol{t}, \boldsymbol{T}_1\right) \qquad \textbf{(2.25)}$$

where $A_x(T_1,T_2)$ and $A_y(T_1,T_2)$ are the shifts in time and amplitude when going from temperature T_1 to T_2. This expression can then be Fourier transformed to get the corresponding shift in the frequency domain

$$\hat{\chi}(\omega,T_2)=\left(\frac{A_y(T_1,T_2)}{A_x(T_1,T_2)}\right)\cdot\hat{\chi}\left(\frac{\omega}{A_x(T_1,T_2)},T_1\right) \qquad (2.26)$$

The function $A_{x,y}(T_1,T_2)$ is most often strongly temperature dependent and can for some dielectric materials be expressed with the Arrhenius factor

$$A_{x,y}(T_1,T_2)=\exp\left(-\frac{W_{x,y}}{k_B}\left(\frac{1}{T_2}-\frac{1}{T_1}\right)\right) \qquad (2.27)$$

where T_1 and T_2 represent starting and ending temperatures, $W_{x,y}$ is the activation energy of the material and k_B is Boltzmann's constant. For materials that are more complex, it is also possible that the activation energy is temperature dependent.

The dc conductivity is also sensitive to temperature changes. Usually the temperature dependence of the conductivity can also be described with the Arrhenius factor with activation energy W_{dc} and a pre-exponential constant σ_0.

$$\sigma_{dc}=\sigma_0\exp\left(-\frac{W_{dc}}{k_BT}\right) \qquad (2.28)$$

3 PRINCIPLES OF MEASUREMENT TECHNIQUES

Diagnostic measurements of high voltage insulation, in for example transformers, cables or rotating machines, can be done either in the time or frequency domains. Today existing commercial diagnostic methods are in time domain measurements of polarisation/depolarisation currents and recovery voltage as a function of time and in frequency domain measurements of capacitance, C, and loss factor, $tg\delta$, as a function of frequency. Parameters that are used to describe a linear, homogenous and isotropic insulation material are in the time domain the high-frequency component of the relative permittivity, ε_∞, dc conductivity, σ_{dc}, and dielectric response function, $f(t)$, and in the frequency domain the complex relative permittivity, $\hat{\varepsilon}(\omega)$, or susceptibility, $\hat{\chi}(\omega)$.

To make reliable diagnostics it is important to understand how well each diagnostic method can characterise a high voltage insulation system depending on the insulation's dielectric response. Further, it is also important to understand the mathematical relations between each diagnostic method and how measured data can be transformed from one method to the other. In this chapter, the three methods mentioned above are presented. It is also shown what type of information is realistic to extract.

3.1 Measurements in time domain

3.1.1 Polarisation and depolarisation currents

To measure polarisation and depolarisation currents is one way in the time domain to investigate the slow polarisation processes, as defined in chapter 2.1. Assuming now that a test object is totally discharged and that a step voltage U_0 is applied at a time $t = t_0 = 0$, the polarisation current through the test object with the geometric capacitance C_0, can be expressed as

$$i_p(t) = C_0 U_0 \left(\frac{\sigma_{dc}}{\varepsilon_0} + \varepsilon_\infty \delta(t) + f(t) \right) \qquad (3.1)$$

where $\delta(t)$ is the delta function originating from the derivative of the applied step voltage at $t = 0$. Two parts basically build up the polarisation current. One part is related to the conductivity of the test object and one part is related to the activation of the different polarisation processes within the test object. In dielectric materials used as high voltage insulation there are many different polarisation processes which all have different time constants widely distributed in time.

When the step-voltage is removed at time t_1 and the object is short-circuited immediately, the depolarisation current flows. This current is built up by the relaxation of the polarisation processes that were activated by the step voltage U_0. The depolarisation current for $t > t_1$ is expressed as

$$i_d(t) = -C_0 U_0 \left(\varepsilon_\infty \delta(t - t_1) + f(t - t_1) - f(t) \right) \qquad (3.2)$$

where $\delta(t - t_1)$ is the delta function originating from the short circuiting at $t = t_1$ (equivalent with application of a negative voltage step).

In Figure 5 polarisation and depolarisation currents measured at U_0 =3 kV for an oil-paper insulated object having geometric capacitance C_0 =144 pF (total capacitance C =640 pF), are plotted against time for charging and discharging periods of t =10^5 seconds [17]. The currents have been scaled with $U_0 C_0$, so that the results are comparable with other insulation systems of different geometry and charging voltage. The measured depolarisation current has a negative sign compared to the polarisation current, but when they are plotted together, the sign is changed on the depolarisation current.

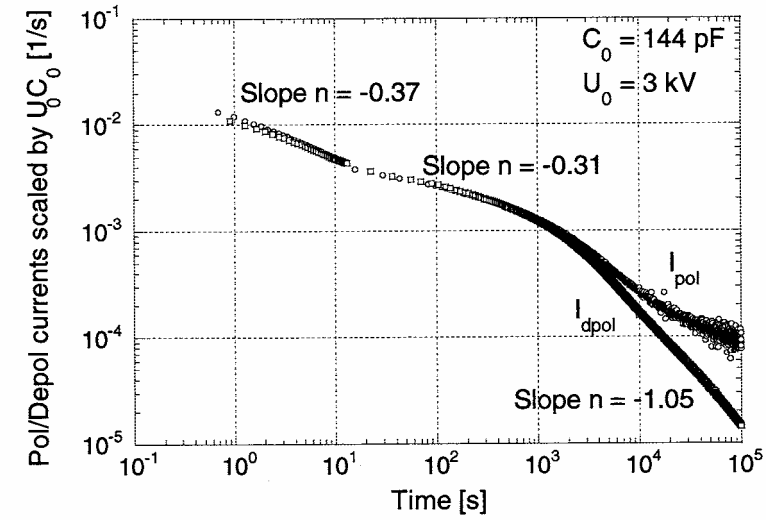

Figure 5 ***Polarisation and depolarisation currents in an oil-paper insulated object, scaled with geometrical capacitance, C_0, and charging voltage, U_0. A clear contribution from dc conduction current is seen in the polarisation current after around 6000 seconds [17].***

The slopes of the currents seen in Figure 5 in the log-log scale are moderate indicating rather slow time dependence. However, there are two break points, the first around 10 seconds and the second around 2000 seconds where the slopes change, indicating a change in the polarisation processes. Around 6000 seconds there is a split up between the charging and discharging currents indicating that the dc conduction current starts to be dominant over the polarisation current.

It is possible to estimate the dielectric response function, $f(t)$, from both the polarisation current $i_p(t)$ and the depolarisation current $i_d(t)$, as can be seen from equations ***(3.1)*** and ***(3.2)***. As the dielectric response function is a continuously decreasing function of time and as the test object can be charged for a sufficiently long time, t_1.

This is probably the easiest way to determine the dielectric response function, $f(t)$, but it is also time consuming from a measurement point of view. There is an approximate rule of thumb which says that the test object should be charged for at least 5 to 10 times as long as the measurement time of the depolarisation current in order to get a depolarisation current which is proportional to the dielectric response function. It is also possible to compensate for the finite charging period, t_1, by trying to estimate the contribution of $f(t+t_1)$ in the equation above. One possible way if doing this is by approximating $f(t)$ for times $t > t_1$ with the t^{-n} behaviour, that is by a curve fit to the last decade of measured data.

It also is possible to estimate the dc conductivity, σ_{dc}, of the test object from the measurements of the polarisation and depolarisation currents. If the test object is charged for $t = t_1$, σ_{dc} can be expressed as

$$\sigma_{dc} = \frac{\varepsilon_0}{C_0 U_0}\left(i_p(t) + i_d(t)\right) - \varepsilon_0 f(t+t_1) \qquad (3.3)$$

It can sometimes be very difficult in dielectric materials to distinguish between true dc conduction and different types of slow polarisation mechanisms. It is important to realise that the test object must be charged until the effects from the dielectric response function have disappeared, $f(t+t_1) << \sigma_{dc} / \varepsilon_0$, in order to get the true dc conductivity.

3.1.2 Return (or recovery) voltage

The recovery voltage method is another method in the time domain to investigate slow polarisation processes. A step voltage, U_0, is applied over the electrodes of a completely discharged test object with geometric capacitance C_0, see Figure 6.

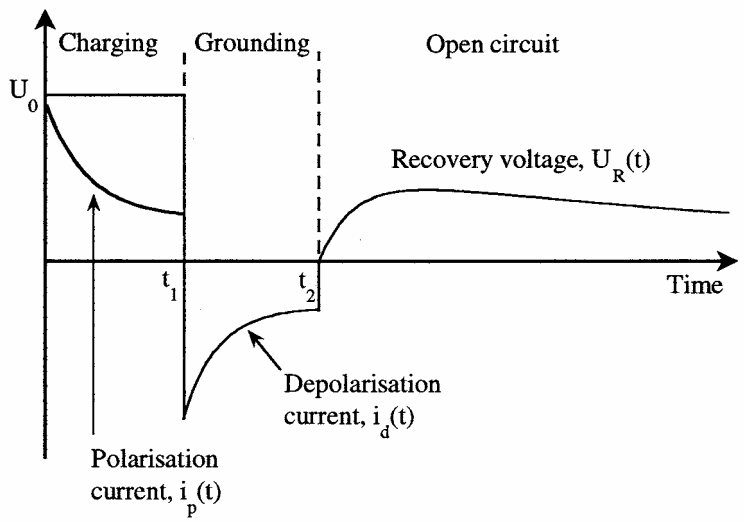

Figure 6 ***During a return voltage measurement the test object is charged with U_0 from $0 \le t \le t_1$, grounded from $t_1 < t \le t_2$ and for $t > t_2$ the recovery voltage is measured at open circuit conditions.***

During the charging period the polarisation current, $i_p(t)$, flows through the test object. After the charging period, the test object is short-circuited (grounded) and the depolarisation current, $i_d(t)$, flows. Both currents are, however, not measured. After the short-circuiting (grounding) period is finished, the return voltage, $U_R(t)$ is measured under open-circuit conditions. The source of the recovery voltage is the relaxation processes inside the dielectric material, giving rise to an induced charge on the electrodes of the test object.

In order to understand why there is a recovery voltage building up during open circuit conditions, the easiest is to look at the current through the test object. The charging period activates polarisation processes in the object. Depending on how long the test object is charged, t_1, different polarisation processes with different time constants become activated. Then during the short-circuiting period, the polarisation processes start to relax. Depending on how long the test object is short-circuited, $t_2 - t_1$, different number of polarisation processes are totally relaxed - totally relaxed means that there is no information left about the polarisation process. Then during the open circuit period the polarisation processes, which were not totally relaxed during short-circuit period, relax further and give rise to a recovery

voltage over the electrodes of the test object. At the same time the recovery voltage re-polarises the object, the polarisation is building up to a degree that is in relation to the magnitude of the recovery voltage. This re-polarisation makes the interpretation of the recovery voltage somewhat difficult. The following equations describe the condition of the recovery voltage build-up

$$\boldsymbol{i_R(t) = \sigma_{dc} U_R(t) + \varepsilon_0 \varepsilon_\infty \frac{dU_{R(t)}}{dt} + \varepsilon_0 U_0 \left(f(t) - f(t - t_1) \right) + \varepsilon_0 \frac{d}{dt} \int_{t_2}^{t} f(t-\tau) U_R(\tau) d\tau = 0} \quad \textbf{(3.4)}$$

for $t_2 < t < \infty$ ***and*** $U_R(t = t_2) = 0$

The forward problem is to calculate the recovery voltage, $U_R(t)$, for a given excitation, knowing the conductivity, σ_{dc}, the high-frequency component of the relative permittivity, ε_∞, and the dielectric response function, $f(t)$. This is a straightforward problem, which can be analytically solved for a dielectric response function that follows the Debye behaviour. For other types of responses the problem can be solved by numerical calculations. The inverse problem is to calculate σ_{dc}, ε_∞, and $f(t)$ from a given recovery voltage, knowing the excitation. This is much more difficult problem than the forward problem and attempts to solve it, by assuming certain analytical form of the response function and then using a non-linear constrained minimisation, were presented recently in [18].

In Figure 7, three different recovery voltage measurements are shown for the same oil-paper insulated object as presented in Figure 5 [17]. It was charged with U_0=500 V for a period of $t_c = t_1$=100, 500, 1000 seconds and every time short-circuited for $t_g = t_2 - t_1$=10 seconds. The solid lines are the numerically obtained recovery voltages (forward problem) from solving equation (3.5) using the dielectric response function, $f(t)$, and dc conductivity, σ_{dc}, estimated from polarisation and depolarisation current measurements.

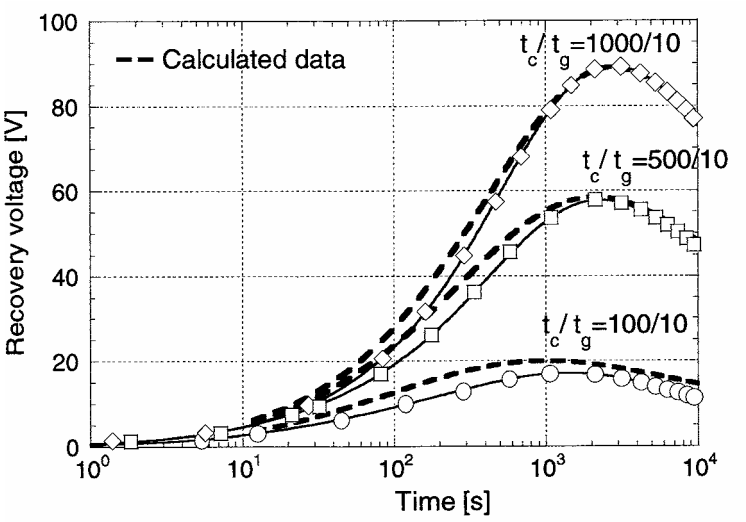

Figure 7 ***Measured and calculated recovery voltage curves for an oil-paper insulated object. Charging voltage U_o=500V was applied for periods t_c=100, 500, 1000 seconds and short-circuiting for t_g=10 seconds. Note the large response and***

the clear influence of conductivity starting to reduce the recovery voltage at around 2000 seconds [17].

3.1.3 The "RVM"-technique

A particular return voltage measurement technique for the on-site measurement of the bulk dielectric properties for power transformers appeared about two decades ago. This method, now called RVM technique was originally proposed in [5] and in succeeding papers (e.g. in [19] and [20]). It became attractive, as it was, and still is, claimed that the moisture content in the pressboard of a transformer's composite insulation system can be quantified by analysing a "polarisation spectrum" evaluated from the measured procedure. This "spectrum" is produced by applying a series of individual charging voltages U_0 to the test object, followed by a short-circuiting period as explained in Figure 6, at each cycle increases of the charging period, $t_1 = t_c$ as well as the short circuiting period, $t_2 = t_g$ are made, when using a fixed ratio of t_c / t_g for the measuring series, usually equal to 2. After t_g has elapsed, the recovery voltage $U_R(t)$, for a particular cycle, is recorded and from its peak value, the amplitude $U_{R\max}$ is quantified with the charging period t_c for that cycle. The resulting curve, $U_{R\max}$ as a function of T_c, is called the polarisation spectrum. The initial derivative, dU_R/dt of the recovery voltage is also found and can be plotted as a function of t_c. However, some users of the "RVM" technique prefer so called "Guuinic signature" plot, in which the dependence $dU_R/dt = f(U_{R\max})$ is represented. Examples of the polarisation spectrum as well as of the signature are shown in Figure 8. These were obtained during RVM measurements on a 600 MVA generator transformer.

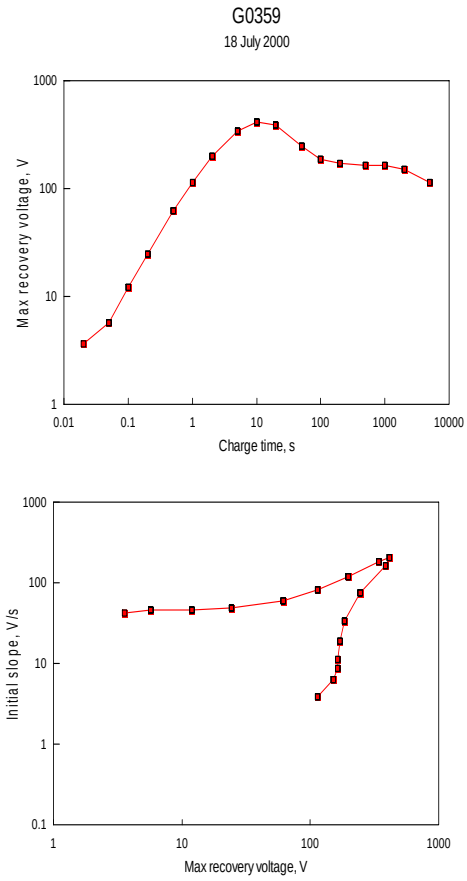

Figure 8 ***Examples of polarisation spectrum*** $U_{R\max} = f(t_c)$ ***and of Guuinic signature plot*** $dU_R/dt = f(U_{R\max})$ ***for a power transformer. Charging voltage*** U_o ***=2000V was applied for periods*** t_c ***ranging from 0,02 to 5000 seconds.***

3.2 Measurements in frequency domain

An equivalent method in the frequency domain to investigate the slow polarisation part is to measure the response from a sinusoidal excitation. Since only sinusoidal excitations are considered, the current resulting can be expressed as follows

$$\hat{I}_M(\omega) = i\omega C_0\left(\varepsilon_\infty + \chi'(\omega) - i\left(\frac{\sigma_{dc}}{\omega\varepsilon_0} + \chi''(\omega)\right)\right)\hat{U}_A(\omega) = i\omega C_0\left(\varepsilon'(\omega) - i\varepsilon''(\omega)\right)\hat{U}_A(\omega) \quad (3.5)$$

On this basis the complex relative permittivity at the frequency of the applied field, assuming a capacitive test object, can be found. It is important to notice that the imaginary part of the complex relative permittivity, $\varepsilon''(\omega)$, (loss part) contains both the resistive (conduction) losses and the dielectric (polarisation) losses. When making the measurement at an arbitrary frequency it is not possible to separate these two components. However, the resistive part is often dominant at very low frequencies. The behaviour of the complex relative permittivity when the resistive losses are dominant is that its imaginary part, $\varepsilon''(\omega)$, has a slope of ω^{-1} and

the real part $\varepsilon'(\omega)$ is constant, see equation (2.16). It is therefore possible to determine the conductivity of the test object from the measured imaginary part of the complex relative permittivity.

Another way of presenting the measured information is to study the frequency dependent ratio between the imaginary and real part of the complex relative permittivity called loss factor, $\boldsymbol{tg}\delta(\omega)$

$$\boldsymbol{tg}\delta(\omega) = \frac{\varepsilon''(\omega)}{\varepsilon'(\omega)}$$

One practical advantage with the use of $\boldsymbol{tg}\delta$ is that it is independent of the object geometry. This makes $\boldsymbol{tg}\delta$ the only possible parameter to study when the geometry of the test sample is not known. However, when the geometry is known, the real and the imaginary parts of the complex relative permittivity, $\varepsilon'(\omega)$ and $\varepsilon''(\omega)$, provide separately more information (conductivity σ_{dc}, high-frequency component of the relative permittivity ε_∞, and dielectric susceptibility $\bar{\chi}(\omega)$). It is also sometimes argued that it is easier to interpret data in the frequency domain than data in the time domain since the frequency data sometimes show nice features, like peaks [9] [21], [22].

In Figure 9, the real and imaginary part of the complex electric susceptibility measured at 3 kV peak are plotted for the same oil/paper insulated object [17] as presented in the previous two sections. Looking at the curves it can be seen that the object has rather high losses, like in the time domain. A strong frequency dependence is present, but it is difficult to distinguish the dc conduction component since the object shows a strong low frequency dispersion (hopping) behaviour at low frequencies, identified by the real and imaginary parts being parallel [9], [23]. Interesting features for oil/paper insulation is the position of the minima in frequency and the slope of the curves in the low frequency dispersion region, which can be related to the temperature of the material [22].

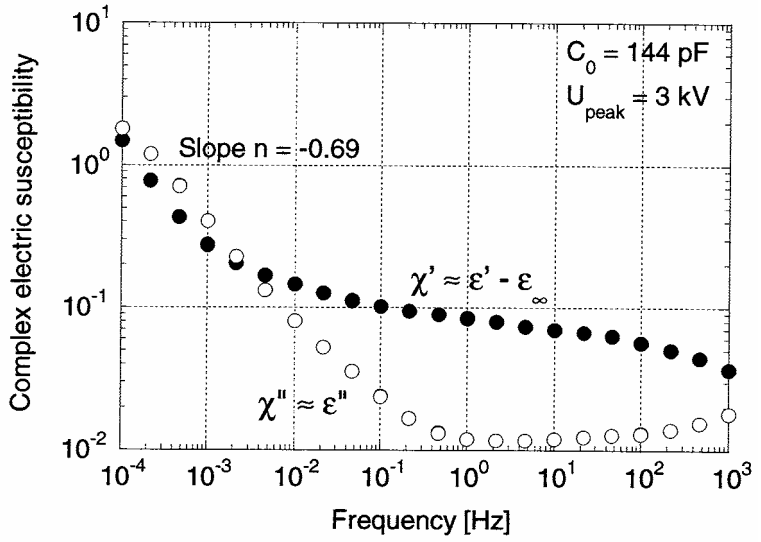

Figure 9 ***Complex dielectric susceptibility of an oil-paper insulated object. There is no clear contribution from dc conduction for the lower frequencies in this frequency window (χ'' and χ' are parallel) [17].***

4 DIELECTRIC BEHAVIOUR OF OIL IMPREGNATED SYSTEM

4.1 Pressboard and oil

In order to understand the behaviour of the whole insulation system of power transformer, consisting of oil and cellulose (most commonly pressboard and paper), information is needed on the dielectric properties of its constituents. Measuring procedures allowing for determining these properties have already been presented in Section 3.

The electrical characteristics of non-impregnated pressboard, such as effective or resultant permittivity, dielectric loss, and conductivity, essentially determine the performance of the final product, i.e. the impregnated pressboard. The structure of non-impregnated pressboard can be considered as a combination of air and cellulose fibres. In microscopic scale, it is a mesh consisting of an infinite number of small channels and filaments having remarkable capillary properties. Such a structure possesses great ability to absorb both gases and liquids. Therefore, pressboard dried under best conditions still would contain small, although definite, amount of water in form of very thin films or layers attached to the surfaces of cellulose fibres. These layers may be considered as limited conducting paths, which contributes to both increase of conductivity and dielectric loss. Both non-impregnated and impregnated pressboard exposed to ambient air absorbs water from it, as the cellulose, a linear polymer whose monomer is glucose, is of hygroscope nature. Depending on the humidity of air to which pressboard (or paper) is exposed, the water content may attain several percents in weight.

The physical processes, as effective for the absorption of humidity to either non- or oil-impregnated pressboard, are well known [24]. To recall a typical example of moisture absorption, only some recent results are reproduced in Figure 10, as taken from investigations performed by Weidmann AG, Switzerland [25]. These investigations, performed on previously dried Transformerboard T IV (250 x 250 mm^2, thickness 1 and 5 mm), have been carried out at 23 °C and relative humidity of 75%. The drying process involved hot air, 4 hours at 90 °C and vacuum treatment (< 2 mbar), for 44 hours at 105 °C. The oil impregnation (if applied) was carried out under vacuum at 90 °C with processed transformer oil. Three individual board samples have been used for each of the measurements and the presented results are mean values. The results are related to the weight increase.

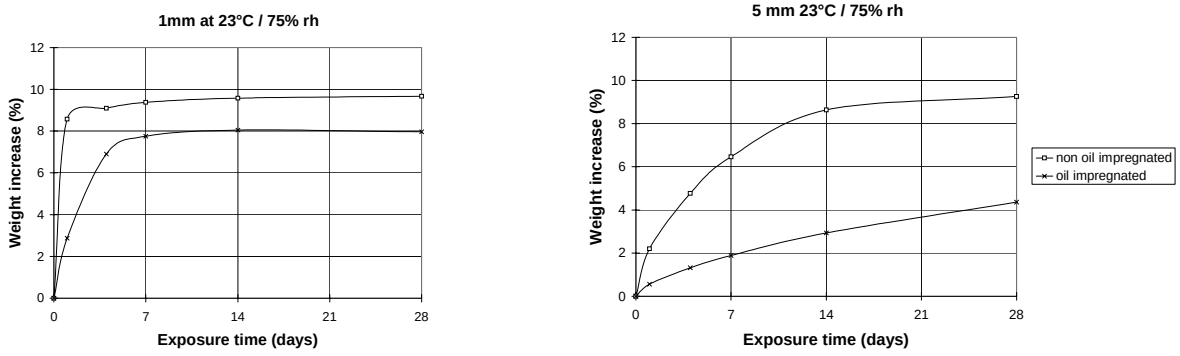

Figure 10 Weight change of dried and dried & oil impregnated Transformerboard T IV samples during exposure to ambient air [25].

The data presented in Figure 10 as well as other similar results revel the following features of the oil impregnation process:

- Oil impregnation of pressboard slows down the water absorption process efficiently, but does not prevent it. For given atmospheric conditions, the equilibrium moisture content is nearly the same for non-impregnated as well as for impregnated pressboard.
- The protective function of oil impregnation is obviously more pronounced for 5 mm board than that for 1 mm.
- Thin samples absorb humidity faster than thicker ones. For non-impregnated 1 mm samples the absorption process lasts hours to days, whereas for the 5 mm sample, the process takes weeks.
- Moisture absorption is dependent on temperature and is somewhat slower for lower temperatures for equal relative humidity. This is consistent with earlier work in which the temperature dependence of diffusion coefficients of non-oiled insulation has been investigated [26].

Moisture in non-impregnated paper has no much influence on the chemical structure of paper itself, unless ageing processes are involved, but it remarkably affects relaxation phenomena (e.g. plasticity of paper) and, by this, its dielectric properties. Dielectric loss of a dry paper can be entirely accounted for by dielectric absorption [27], [28]. For low moisture contents, very few ionic paths may exist through paper wall and subsequently conduction is very low. Increase in moisture produces a number of additional ionic paths from electrode to electrode resulting in higher conduction. For the power frequency, the permittivity of pure cellulose at 20 °C is 5.6, whereas permittivity of dry paper varies in a range of 1.5 to 3.5 and that of dry, oil impregnated pressboard may range between 3.1 and 4.5 at 20 °C, depending on the density of the board. The loss factor of dry non-impregnated pressboard measured at 50 Hz lies close to 0,003 - 0,004 and it is mainly due to dielectric absorption. Pressboard in dry state exhibits high values of volume resistivity, which can be between 10^{13} and 10^{15} Ωm [29]. One should note, however, that all values are not only dependent on the actual density of the paper or pressboard, but also on the origin, processing and manufacturing procedures of the cellulose and its products.

Contrary to cellulose, mineral oil has very low affinity to water. Oil ability to absorb water depends on the temperature, the chemical structure and its mechanical contamination, especially by cellulose fibres [30], [31]. Naphtenic and paraffinic oils absorb less water than aromatic ones. Water in oil can appear both in solution and in dispersed state (emulsion). Influence of dissolved water on dielectric properties of mineral oil is rather weak and, for example, it has only a weak effect on the dielectric strength as long as the ***relative*** water content is low. Under homogeneous field conditions, the breakdown field strength is at least 30 kV/mm in a temperature range of 20 to 100°C and a water content of less than 5 ppm and the reduction of this value is moderate up to about 20 ppm, even at room temperature. The reduction of dielectric strength is basically only dependent on the relative humidity in insulating oils, i.e. the water content with respect to its ability to dissolve water. It follows, in a limited range of temperature, an exponential law in the form of $\boldsymbol{w} = \boldsymbol{A}\exp\left(-\boldsymbol{B}/\boldsymbol{T}\right)$, where $\boldsymbol{A}$ and $\boldsymbol{B}$ are constants and $\boldsymbol{T}$ is absolute temperature [30]. However, excess of water beyond solubility limit is instantly accompanied by a reduction of dielectric strength to values of about 5 kV/mm [30], [32], [33].

Dielectric loss of mineral oil is mainly due to ionic conduction. Addition of polar molecules (for example, water), ionic compounds (acids and ageing products) as well as mechanical contaminants greatly increases oil conduction and, subsequently the dielectric losses. This increase in conductivity is, however, negligible for water content of up to about 20 ppm [30], [34], [35]. Conductivity and dielectric loss factor for power frequencies are also dependent on field strength in a quite non-linear manner [30], [36]. The dielectric dispersion of transformer oil is negligible in the range of times and frequencies of interest here. The power frequency permittivity value, $\varepsilon \approx 2.2$, and its specific dc conductivity, σ_{dc} can simply describe its dielectric response. It is important to stress that the conductivity of oil can vary broadly depending on content of different contaminating products and therefore can significantly influence the dielectric response of the whole insulation system. The temperature dependence of the conductivity is characterised by activation energy of ca. 0.4 to 0.6 eV [37], which is significantly lower than that of oil-impregnated pressboard.

It is often assumed that the response of oil is linear. For field work on aged transformers this is generally the case, something that have been verified many times. For new transformers the ionic charge carriers may be swept out of the gaps (electrostatic cleaning effect) so that the oil becomes less conducting [38], [39]. This non-linear effect may be more or less reversible. The best way to avoid these effects [U. Gfvert and H. Kols: "Simple method for Determining the Electrical Conductivity in Transformer oil", Conf. Record of Nordic Insulation Symposium, Helsinki, Finland, June 9-11, 1986, p.23:1] is to use as low voltage as the noise level allows [40].

4.2 Dielectric response of insulation system components

Dielectric response functions in time domain can be deduced directly from the depolarisation currents as already shown in Section 3.1. Examples of response functions obtained for a typical insulating oil, oil-impregnated and non-impregnated pressboard containing different moisture content and, for oil-impregnated pressboard, of different degree of ageing will be shown in the following sections. It must be emphasised however that response functions, at least in the very long times, i.e. longer than seconds, are quite sensitive to e.g. temperature, material composition, and test conditions.

4.2.1 Dielectric response of mineral oil

As already mentioned before and recently confirmed by measurements of dielectric response on oil samples [41], the dielectric dispersion in oil can be neglected within the frequency range of interest, i.e. for frequencies approximately equal to or lower than power frequency. This statement can be confirmed by results shown in Figure 11. Here, the polarisation as well as the depolarisation currents is shown for a sample of new (unused) mineral oil (Type Technol US 3000) in dependence on increasing charging duration. The measurements were made by applying dc voltage of 10 V to a 2 mm oil gap in a test cell with parallel plate electrodes and guard ring. The measurements started with a sequence of 100 s voltage application (polarisation current) and immediately afterwards short-circuiting (depolarisation current). The next sequences (1500 s and more) followed after a longer short circuit time. The initial high amplitudes of polarisation currents and their transition to low values, which were not dependent on the preceding measuring sequence, were due to the motion of charge

carriers (ionic impurities) within the gap, which started from their initial positions and moved to the electrodes. The drift velocity of these charge carriers is dependent on the amplitude of the voltage applied. This means that the transition part of the polarisation current will be shifted to shorter times by increasing the excitation voltage level. The final value of the polarisation current is obviously governed by a continuous ion formation.

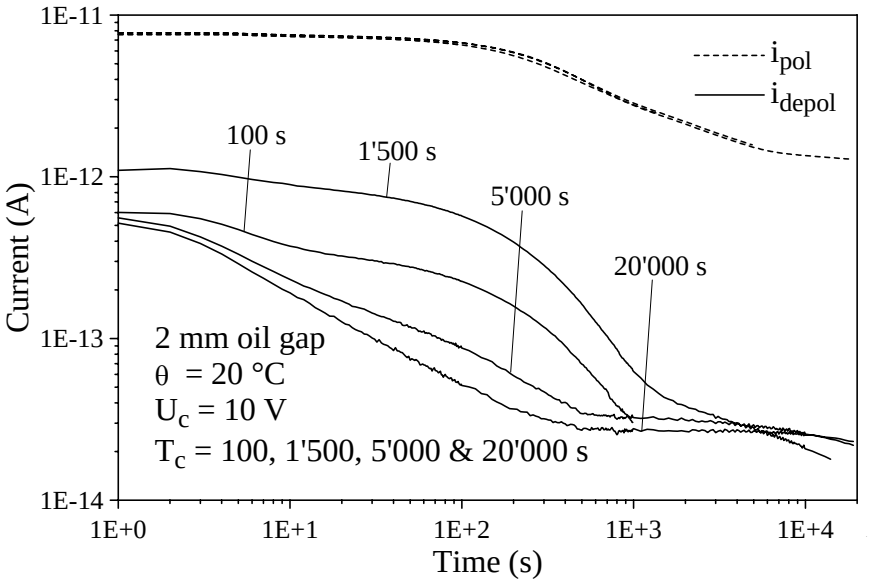

Figure 11 Polarisation and depolarisation currents of a new (unused) mineral oil sample for different duration of charging period [41].

The amplitudes of depolarisation currents are much smaller than those of the polarisation currents. They decreased, for charging duration higher than 1500 s, after each additional period of voltage application. This effect is obviously due to a reduction of a part of the charge carriers at the electrodes after each excitation. These responses of oil to dc voltages applied show that the currents generated for times > 1 s are mainly due to the motion of charge carriers. Therefore, they differ fundamentally from relaxation current, which can be observed in solid dielectrics.

The polarisation currents in Figure 11 demonstrate that the apparent conductivity of oil changes continuously with the application of a dc field, i.e. $\sigma_{dc} = \lim_{t \to 0}(j/E)$. The values determined at short times correspond to the conductivity values determined with ac or combined low voltage/low frequency methods [42], [43], [44]. This effect is also verified for the sample presented here. From a measurement performed with a 0,02 Hz triangular voltage wave of 15 V_{pp}, a conductivity of 1.42×10^{-13} S/m was determined. This value corresponds to a conductivity value, which can be evaluated from the polarisation current after 28 s of dc voltage application.

This investigation confirms that the dielectric dispersion of transformer oil is negligible in the range of times and frequencies of interest here, i.e. the dielectric response function $f(t)$ for times higher than 1 s can be assumed as zero. Therefore, for all investigations in this work the oil is characterised by its relative permittivity at power frequency (about 2.2), its actual or simulated conductivity and its activation energy, which describes the temperature dependence of conductivity. The relative permittivity of oil at power frequency decreases somewhat with

increasing temperature. For temperatures above 0 °C, this decrease is mainly due to the volume expansion of oil [45], [46].

4.2.2 Dielectric response of oil-impregnated pressboard

The measurements have been performed on homogeneous test samples by placing 2 mm thick impregnated pressboard samples (Weidmann Transformerboard Type T IV, impregnated with Technol US 3000 mineral oil) in a parallel-plate test cell with stainless steel electrodes. The diameter of the guarded electrode from which the relaxation currents have been extracted was 113 mm. The geometric capacitance $\boldsymbol{C}_0$ for a gap distance of 2 mm was thus 44,4 pF. The electrode arrangement was placed in an oil-filled glass vessel. The magnitude of the applied polarisation voltage was restricted to 200 V (field strength of 100 V/mm) to avoid non-linear effects [41].

The results presented refer either to virgin (non-aged) or aged pressboards with moisture contents (m.c.) as indicated in Figure 12 and Figure 13 below. The m.c. of a sample was defined by the percent ratio of water weight absorbed from the sample to its dried and non-impregnated weight. "Complete dryness" was accepted to coincide with a m.c. of about 0.2 % which can be reached by a drying procedure under vacuum (< 1 mbar) for 24 hours at 105 °C. Larger moisture levels were reached and controlled by exposing the samples to ambient air and a weighing procedure. After reaching the desired m.c., the samples were stored (hermetically sealed) for one week before impregnation. The impregnation was performed with the degassed and dry oil with moisture content of 5 ppm under ambient air pressure. Figure 12 shows the polarisation and depolarisation currents for some virgin, non-aged samples at U_0 = 200 V with different m.c. [41]. The currents are plotted against time from 1 s after step voltage application and short circuit respectively up to the very long measurement periods of 200000 s. The different dielectric response functions, $\boldsymbol{f(t)}$, as already defined in Section 3.1, can simply be scaled by dividing the current amplitudes by the product of geometric capacitance, $\boldsymbol{C}_0$, and the applied step voltage of 200 V (i.e. by a factor of $88{,}8 \cdot 10^{-10}$ As).

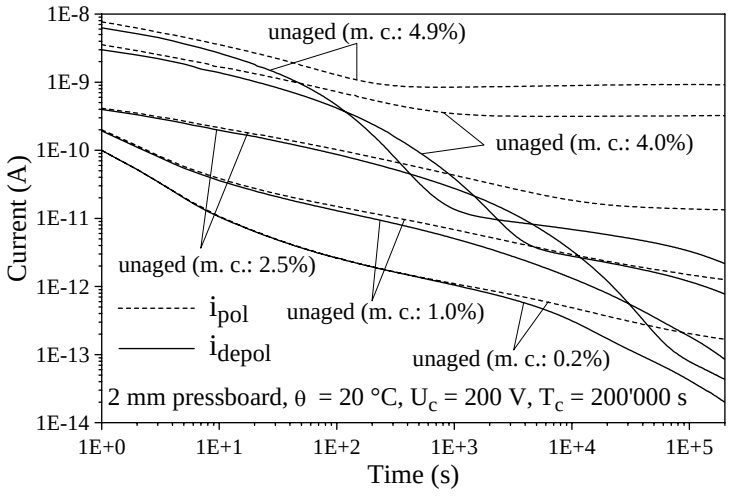

Figure 12 Relaxation currents (polarisation, i_{pol}, and depolarisation, i_{depol}) of unaged samples with different moisture content. Duration of polarisation and depolarisation was 200000 s each [41].

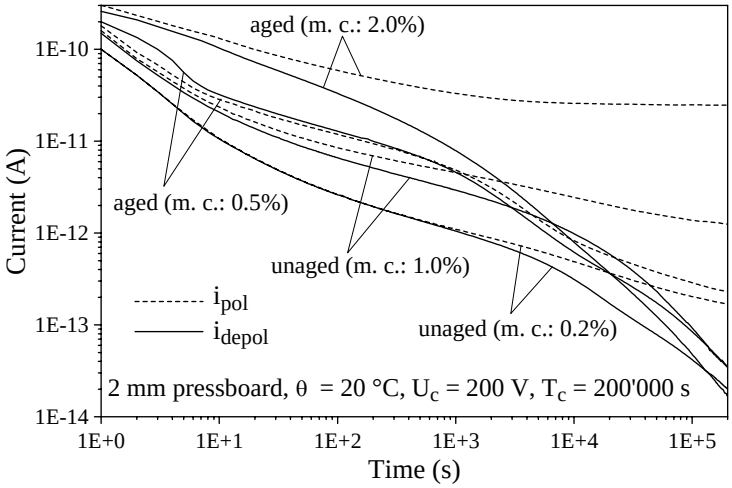

Figure 13 Relaxation currents of pressboard samples before and after ageing [41].

It appears obvious that the response functions are strongly dependent on moisture content. The magnitudes of the conduction currents can best be identified after a split-up of both currents, as the logarithmic scale is not able to identify these differences as long as the current amplitudes are still large (see also Figure 5). The main differences of the shapes are obviously caused by the statistical distribution of the (microscopic) interfacial polarisation phenomena within the complex structure of the pressboard. The individual "high frequency" components of the relative permittivities of the samples, which are also dependent on moisture content have been measured at power frequency of 50 Hz to be 4,1, 4,5, 4,8, 5,1 and 5,3 respectively for the increasing m.c. values of 0,2, 1,0, 2,5, 4,0 and 4,9 %. In summary, all dielectric response function show large dielectric dispersion within this time period.

Results of measurements on similarly prepared samples in frequency domain are shown in Figure 14. They exhibit clearly dispersive behaviour, especially at low frequencies.

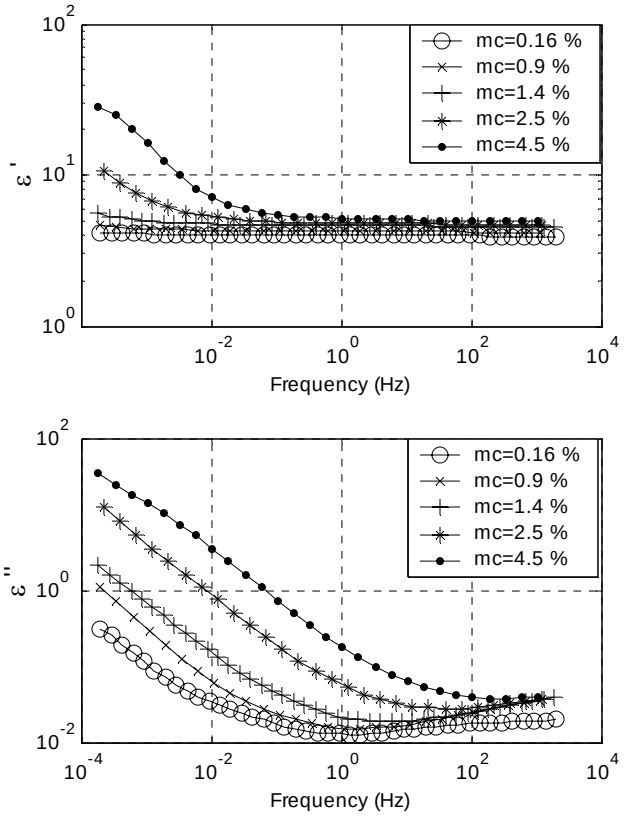

Figure 14 ***Real, ε' and imaginary, ε'' components of the complex permittivity as a function of frequency at 27 C for pressboard samples containing different amounts of moisture [47].***

Samples with an initial moisture content of 0,2% and 1,0% have also been artificially aged for 90 days in a hermetically sealed stainless steel vessel at a constant temperature of 120 °C (weight ratio oil to pressboard: 8,4). This kind of ageing process increased the moisture content of the pressboard, now determined by Karl Fischer titration, from 0,2 to 0,5 % and from 1,0 to 2,0%, respectively. During this ageing process, the moisture content of the oil within the vessel increased to 9 ppm and 19 ppm, respectively. The degree of polymerisation (DP-value) during ageing changed from an initial value of 950 to 479 and 195, respectively, which confirms the effectiveness of the artificial ageing.

In Figure 13 the virgin and aged samples are compared. The increase in moisture content due to the applied ageing procedure, i.e. from the unaged states of 0,2 % and 1 % to the aged states of 0,5 % and 2 % respectively, can well be seen from the relaxation currents. The current amplitudes of the aged samples were significantly larger within the first three decades of time in comparison to those of unaged samples. Furthermore, the relaxation currents of the samples with initially low moisture content were less affected than those with an initially higher one. Ageing products other than humidity obviously contribute to the fist part of the depolarisation currents of the aged samples, but the influence of humidity to the conductivity is dominant. No endeavours have been made to identify such other ageing products by chemical analyses.

As all kinds of dielectric response measurements are sensitive to the influence of temperature, the behaviour of an unaged sample at 5, 20, 35 and 50°C have been studied in frequency as

well as in time domain [41]. The time domain measurements are reproduced in Figure 15, in which the results are presented of the sample with m.c. of 2.5 % in dependence on temperature under conditions as indicated in the figure. According to the theory of Fourier transforms, a horizontal shift in frequency domain corresponds to a shift along a line with a slope of -1 in the double logarithmic plot in time domain.

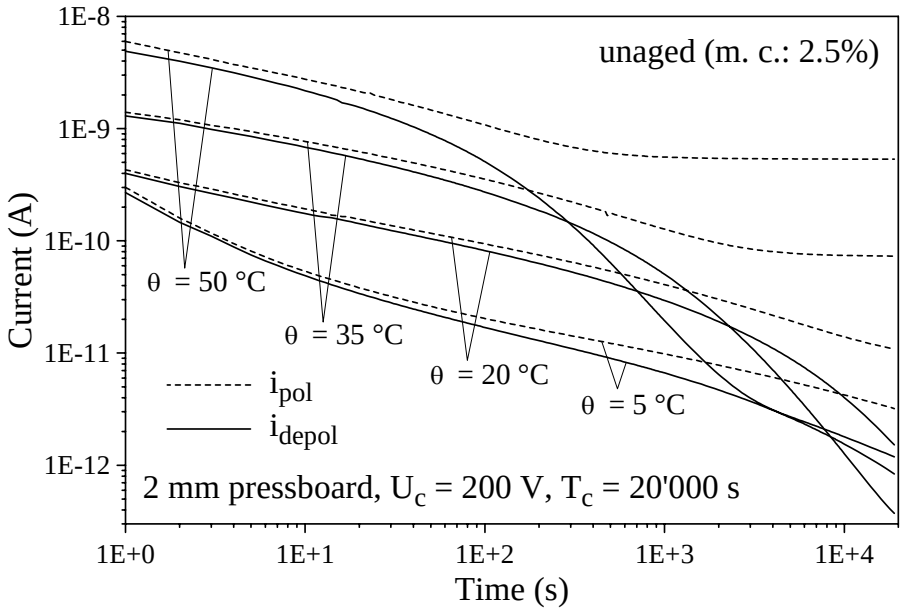

Figure 15 Temperature dependence of the relaxation currents of pressboard sample with 2.5 % moisture content [41].

Figure 16 shows the "master curve" of depolarisation current at 20 °C of the same sample as in Figure 15. To minimise the influence of limited charging duration, new depolarisation currents with a hypothetical infinite charging duration have been calculated from relevant equivalent circuits, derived from the measured depolarisation currents. Only the initial values up to 2000 s have been shifted along the line with slope of -1 until coincidence was attained.

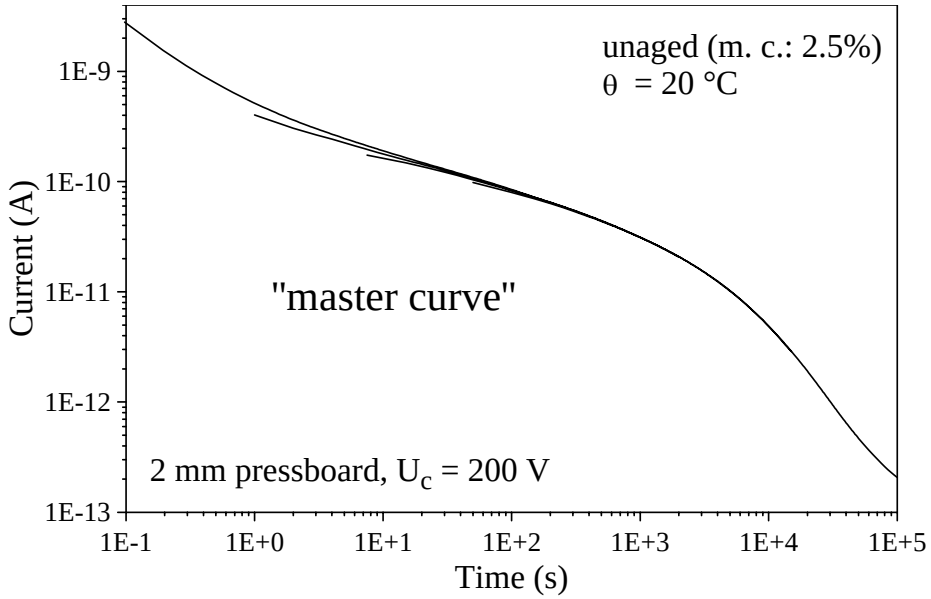

Figure 16 ***"Master curve" of depolarisation current, obtained from shifting the depolarisation currents of Figure 15 [41].***

Similar principles apply to temperature shift in frequency domain. Master curve can be obtained as illustrated in Figure 17.

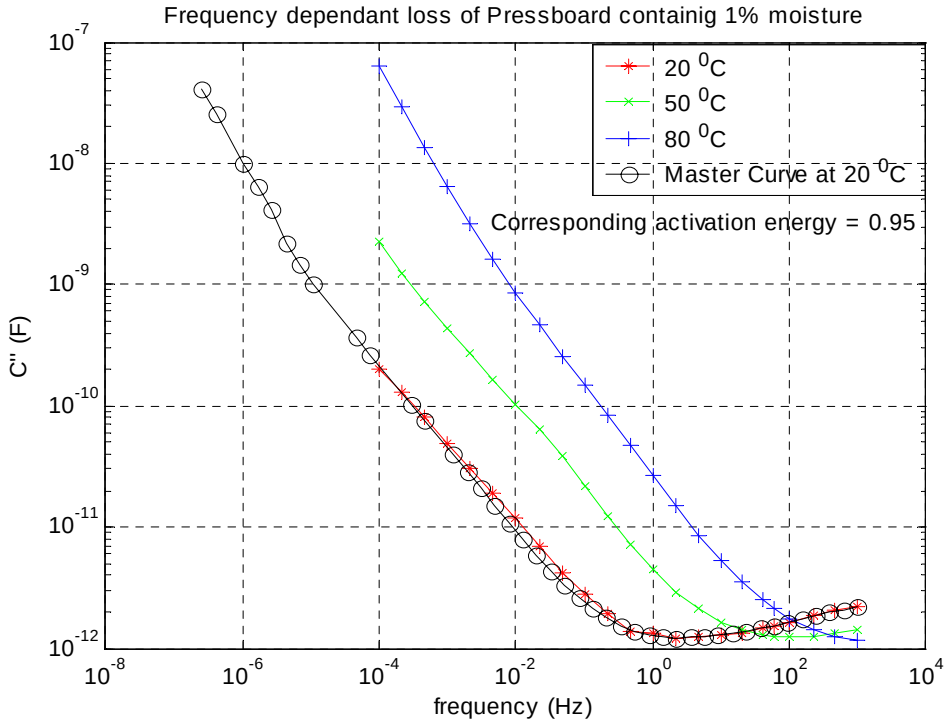

Figure 17 ***Frequency dependence of dielectric loss measured at different temperatures on pressboard sample containing 1% of moisture and the corresponding "master curve".***

As already known from equation ***(*** 2.27***)*** the temperature dependence of the dc conductivity of pressboard obeys a quasi-exponential law. Therefore, the dependence can be characterised by

its activation energy. Figure 18 presents the Arrhenius plot of the logarithmic shift for the same sample. Thus the activation energy for dielectric loss can be calculated from the slope of the fitted line and it is here equal to 1.07 eV. The investigations showed that this activation energy as well as that for the dc conductivity can be slightly augmented by the increase of moisture content.

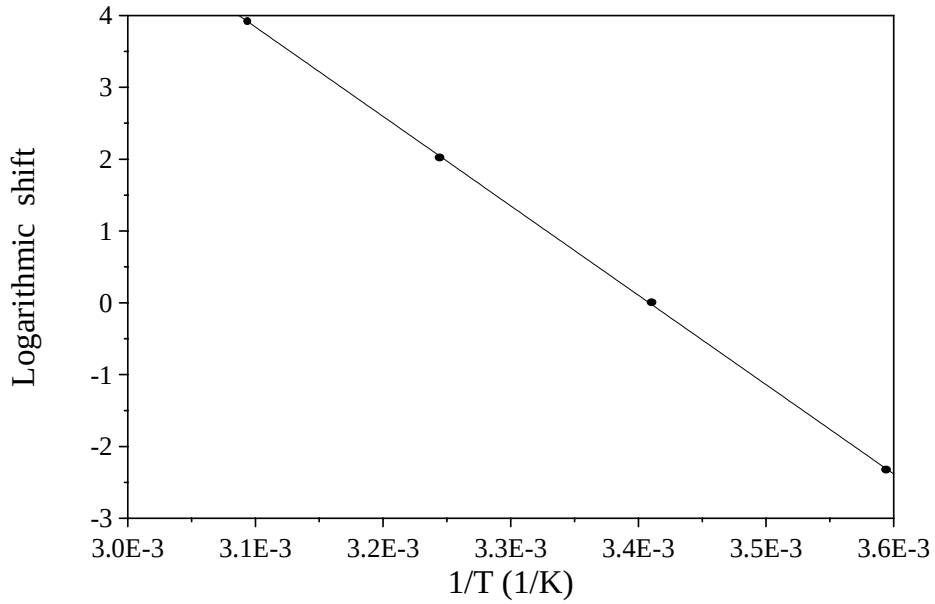

Figure 18 Logarithmic shift as a function of temperature: Arrhenius plot [41].

4.2.3 Summary and conclusions

It has been shown that oil and pressboard have quite different dielectric response functions or dielectric properties. The dielectric response of mineral oil is quite simple and can be characterised by essentially its permittivity and conductivity as dielectric dispersion can be neglected. Pressboard is characterised by large dielectric dispersion, which is in addition dependent on moisture content and ageing products. If both components are sandwiched, the resultant dielectric response function becomes quite different from those of its individual components. It is shown later in chapter 5, that it is possible to calculate the resultant function based on modelling procedures.

Though not shown here in detail, the responses of these materials are linear with respect to electric field stress if the magnitudes are low. If the response is linear, we can also calculate the dielectric response function $f(t)$ from the frequency domain data and vice versa. In order to avoid the influence and difficulties caused by presence of the dc conductivity, one often make use of the frequency dependence of the real part of the permittivity ε'. The agreement between the response functions obtained in both ways, i.e. from the time domain and frequency domain responses, is usually good. Only at highest moisture contents (>3%) the agreement is not so good and it is likely that non-linear effects of electrochemical nature (battery effects) are important for the highest moisture contents [48]. Similar effect has also been observed in oil-impregnated papers for high voltage cable insulation [49].

5 SIMULATION OF DIELECTRIC RESPONSE IN POWER TRANSFORMER INSULATION

To make a precise moisture estimation of the oil-paper insulation in a transformer one needs a library containing data on dielectric properties $\varepsilon_\infty, \sigma_{dc}$ and $f(t)$, of well characterised materials (oils and impregnated pressboard) at different humidity content. This information is needed for calculating the dielectric response of the composite duct insulation and for comparing it with results of the measurements. It is important to note that, depending on the coupling of the transformer windings, different combinations of insulation may influence the measurement. Therefore one also needs information about the geometrical design of the transformer insulation. In Figure 19 a typical winding configuration of one phase of a power transformer is shown.

When current measurements are performed, in both frequency (FDS) and time (PDC) domains, typically the current sensing instrument is coupled to the low voltage winding (Winding A in Figure 19) and the voltage supply is connected to the high voltage winding (Winding B in Figure 19). In the simplest case the part of the transformer as "seen" by the instrument is only the main duct between the high and the low voltage windings, A-B duct. The outer B-C duct to the third winding (Winding C) is not "seen" by the instrument. If, on the other hand and as it sometimes happens, Winding C is situated on the other side with respect to Winding A and it is connected to the high voltage winding (Winding B), then the measurement is performed on both the A-B duct and the B-C duct connected in parallel.

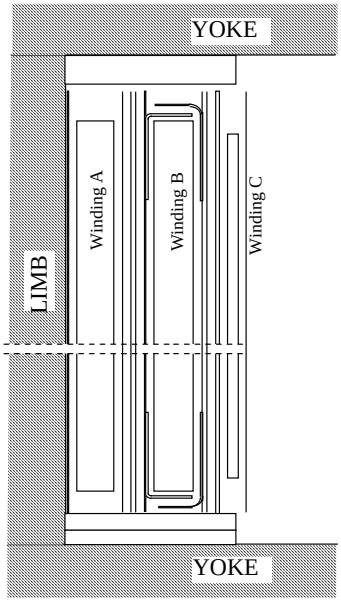

Figure 19 Schematic drawing of winding configuration of a power transformer.

On the other hand, in the typical RVM measurement [50] the instrument may be connected to Winding A whereas the other windings are grounded. Then the object sensed is the insulation duct between the core and the A-winding in parallel with the main duct insulation in the A-B duct, as shown in Figure 20. In addition, as also the bushing connecting Winding A to the high voltage source is involved, the insulation system of this bushing (both its internal and

external parts) is again in parallel to the main duct insulation and thus becomes a part of the system measured.

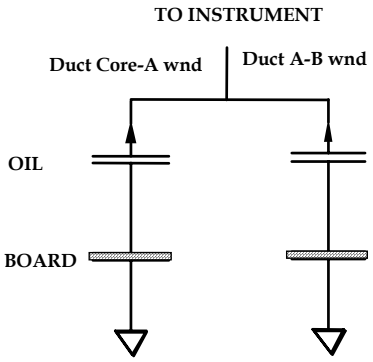

Figure 20 Symbolic circuit representation of the insulation seen by a recovery voltage measurement.

In a current measurement the magnitude of the current depends on the size of the transformer. To represent the size of the transformer one uses the geometric capacitance between the windings, $\boldsymbol{C}_0$, which is simply the capacitance as if the transformer contained not the composite insulation, just air or vacuum only.

For a core type transformer the geometric capacitance $\boldsymbol{C}_0$ is well estimated by the capacitance between two concentric cylinders.

$$\boldsymbol{C}_0 = \frac{\varepsilon_0 \cdot 2\pi \cdot \boldsymbol{h}}{\log(\boldsymbol{r_B} / \boldsymbol{r_A})} \qquad \textbf{(5.1)}$$

where $\boldsymbol{h}$ is the (average) winding height, $\boldsymbol{r_A}$ and $\boldsymbol{r_B}$ are respectively the inner and outer radius of the insulation between the windings. In practice, the geometric capacitance can be estimated by measuring the capacitance between the measurement electrodes at power frequency and then by dividing it by the effective permittivity of the combination of materials. For shell type transformers, it requires some more work to calculate the geometric capacitance, $\boldsymbol{C}_0$, however for those who are familiar with shell type designs this should not represent major difficulty.

In a core type transformer the main insulation usually consists of a number of cylindrical shells of pressboard barriers, separated by axial spacers, as illustrated in Figure 21.

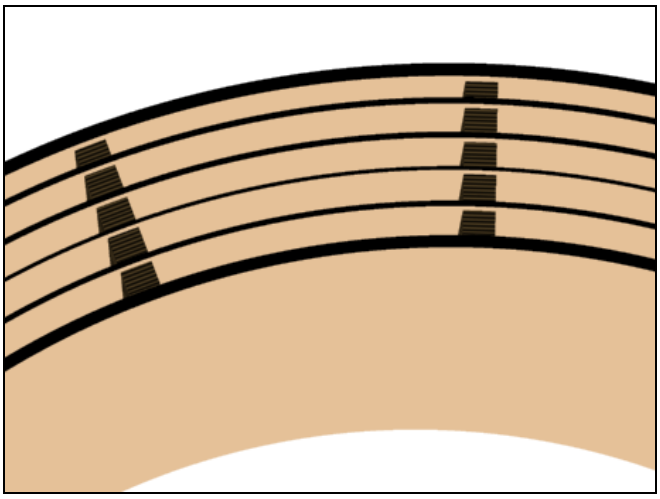

Figure 21 Section of an insulation duct of a power transformer with barriers and spacers, seen from above [6].

For modelling purposes it is sufficient to represent the insulation structure by the relative amount of spacers and barriers in the duct. We define, as it is indicated in Figure 22 a parameter, $\boldsymbol{X}$ as the ratio of the sum of all the thickness of the all the barriers in the duct, lumped together, and divided by the duct width. The spacer coverage, $\boldsymbol{Y}$ is defined as the total width of all the spacers divided by the total length of the periphery of the duct.

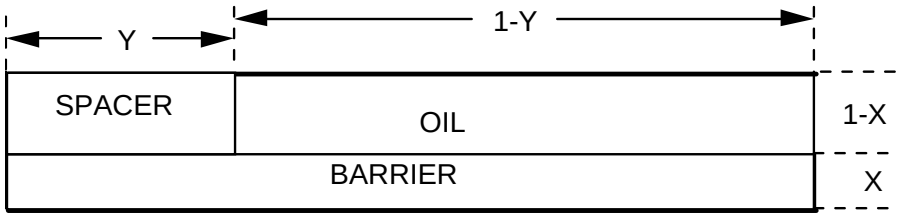

Figure 22 Schematic representation of the barrier content and the spacer coverage in the insulation duct [6].

The range for the relative barrier amount $\boldsymbol{X}$ is typically 0.15 to 0.5. The relative spacer coverage $\boldsymbol{Y}$ is typically 0.15 to 0.25.

From the library of data on material properties and the geometry of the composite system, the PDC, RVM and FDS responses can be derived. In time domain (PDC and RVM methods), the calculation is based on the known response function, ***f(t)***, and its dependency on temperature and humidity. In frequency domain (FDS method), the composite dielectric permittivity, ε_{duct}, of the insulation duct is calculated as

$$\varepsilon(\omega,T)_{duct} = \frac{Y}{\frac{1-X}{\varepsilon_{spacer}} + \frac{X}{\varepsilon_{barrier}}} + \frac{1-Y}{\frac{1-X}{\varepsilon_{oil}} + \frac{X}{\varepsilon_{barrier}}} \qquad (5.2)$$

where the permittivities of the oil, spacers and barriers are also complex quantities dependent on frequency, temperature and humidity.

Examples, where results of simulations as described above, can be found in [41, 51, 52, 53].

6 STUDY CASES

6.1 Pancake model

A so-called pancake model of transformer insulation was developed for a systematic study on factors that influenced the dielectric properties of a composite oil-paper insulation. The model allowed a systematic study of following factors: (i) test voltage level, (ii) insulation geometry, and (iii) oil quality (conductivity).

The pancake model was built at ALSTOM-Vénissieux (France), using commonly used paper, Kraft Thermo 70, and Nynas Nytro 10GBN insulation oil. The model contained 8 pancake shaped coils (A-H) with ducts containing different amount of oil and pressboard between them (from 85/15 to 0/100 oil/pressboard ratio).

Comparative measurements with the different dielectric response methods were performed at 3 different occasions:

- Stage 1 - shortly after delivery of the model in summer 1999.
- Stage 2 - after a heating of the model to 65 °C, performed within 2 months in November/December 1999.

Stage 3 - shortly after a replacement of the originally applied oil (Nynas Nytro 10GBN) with a less conducting oil (Shell Diala D).

The following figures (Figure 23, Figure 24, Figure 25, Figure 26) show the model and its design.

Figure 23 View of the pancake model during measurements.

Figure 24 View of pancake coil of the model.

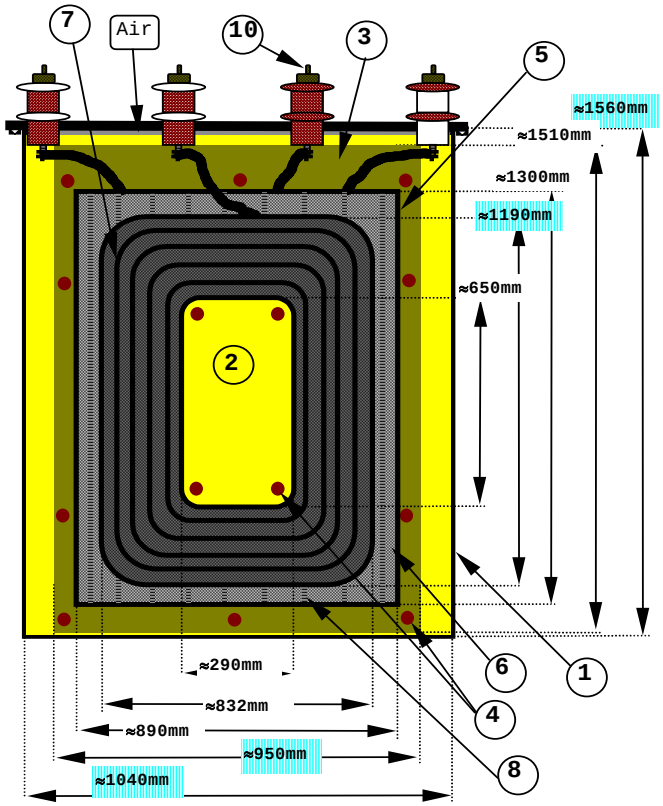

Figure 25 Front cross-section of the pancake model. The marked elements are: 1 – tank, 2 – oil, 3 – bakelite plate, 4 – bakelite rod, 5 – copper plate, 6 – pressboard, 7 – pancake coil, 8 – spacer, 9 – copper band, 10 – connection (bushing).

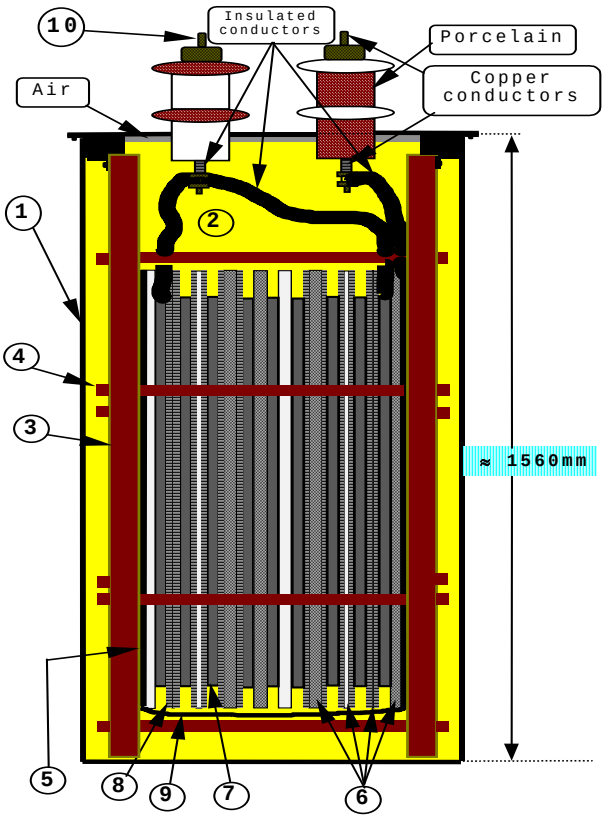

Figure 26 Side cross section of the pancake model.

6.2 Diagnostic measurements

Below some typical and instructive results from the PDC, RVM and FDS measurements are presented. In Figure 27 examples of the measured relaxation (polarisation and depolarisation) currents are shown for the geometrical arrangement of the duct marked 85/15 ratio of oil/pressboard. The moisture content of the insulation studied was estimated to be below 1% using a modelling procedure similar to the one described in Chapter 5. It can clearly be seen how exchanging the oil with one of lower conductivity reduced the polarisation and depolarisation currents early in the measurement, while for longer times dominated by the unchanged pressboard the currents remained unchanged. The results of RVM measurements on different geometrical arrangements and at different times represented as the polarisation spectra and the so-called “Guuinic representation”, in which the initial slope is plotted against the peak recovered voltage, are shown in Figure 28. The interpretation, as provided by the software of the Tettex RVM instrument [4] suggested moisture content of about 2 %. Examples of the FSD results, as obtained in the first stage of the study, are shown in Figure 29. We see that without oil duct there is no peak in the loss factor plot. Based on these results the moisture content in the pressboard was evaluated to be below 1 %. Also this evaluation was – like for the PDC measurements - based on the model presented in Chapter 5. The modelling allowed also for estimating the oil conductivity, which agreed well with results of separately performed measurements according to IEC 61620.

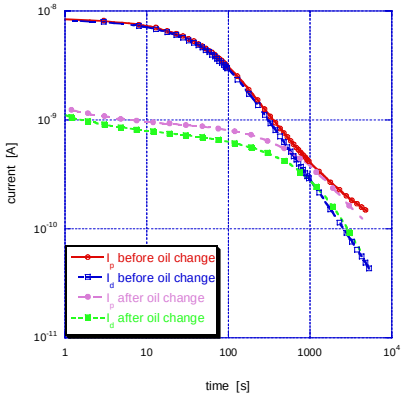

Figure 27 ***Polarisation and depolarisation currents (PDC) as measured on the pancake model before and after oil change; measured geometrical configuration wasmarked as 85/15 oil-pressboard ratio. Full lines are used for the depolarisation currents, and dashed ones for the polarisation currents.***

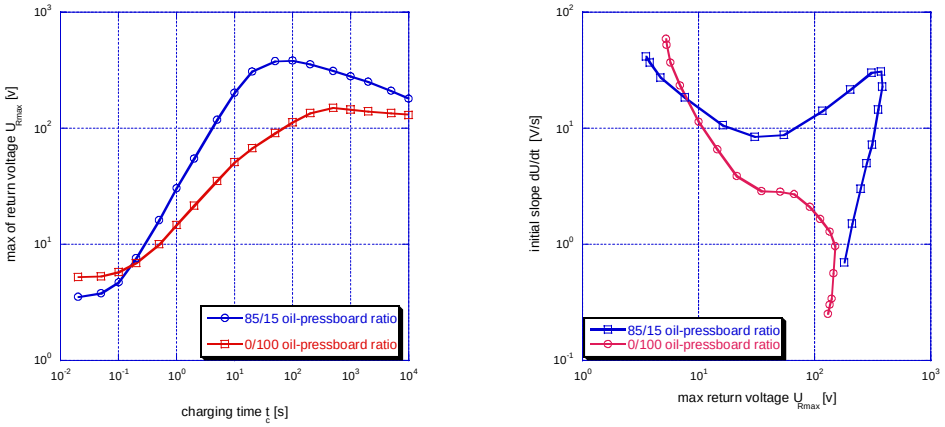

Figure 28 ***RVM polarisation spectra (left) and dU_R/dt plot (right) for two different geometrical arrangements of the coils in the pancake model as measured at 2000 V during the first stage of the study.***

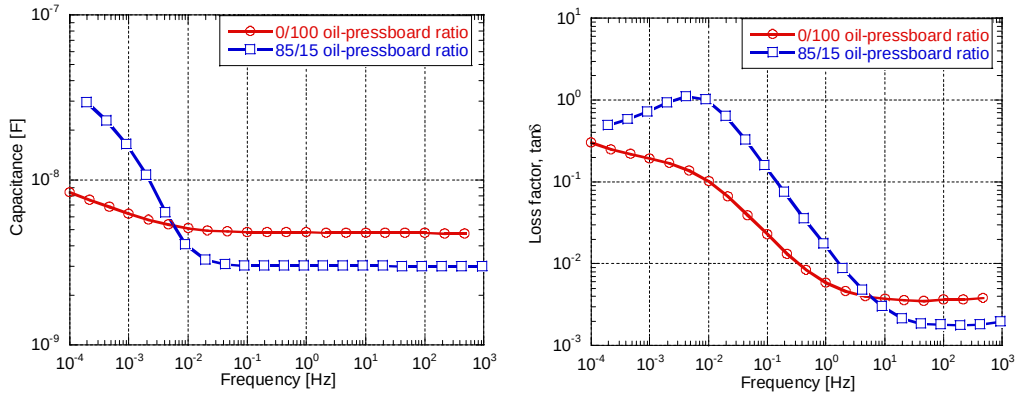

Figure 29 Capacitance (left) and loss factor (right) as a function of frequency of different geometrical arrangements of the coils in the pancake model as measured at the first stage of the study.

In order to elucidate the origin of the discrepancy in moisture evaluation between the RVM measurements and the other methods, stage 2 was introduced, before which the model was kept at 65 °C for two months. It indicated that the oil conductivity was the main cause of the experienced difference. To clarify this further the oil in the pancake model was exchanged with new oil (Shell Diala D) with a much lower conductivity and loss.

The oil change led to a significant modification of the measured responses. This shows how important is taking the oil conductivity into account when interpreting results from the dielectric response measurements on oil-paper insulation systems. A complete documentation of the investigations here referred to will later be published in a special brochure.

To summarise the presented results one may say that the dielectric response measurements on oil-paper insulation are sensitive not only to the state of paper, but also to the oil conductivity and the geometry of the test object. As shown, a risk for errors in the interpretation of the RVM data exists when these parameters are disregarded, resulting in overestimates of the water content. This may especially be of importance when making measurements on new or relatively new transformers in which oil conductivity is unusually high. In a new transformer there will not usually be moisture balance between the oil and the pressboard. The oil is comparatively wetter and will with time be dried out by moisture absorption in the cellulose. This results in a decrease in the conductivity of the oil. Furthermore, results from measurements on transformers with unconventional design (non-typical oil/paper ratios in the insulation) should also be treated with a great care.

6.3 Field measurements

In parallel with the investigations on the pancake model, measurements were also made on real transformers. At National Grid Company (NGC), UK the objective was to investigate the influence of oil condition on dielectric responses to find how this might interfere with any estimation of the water content of the insulation [54]. RVM measurements made before and during an attempted dry-out of a 29 year old 400/132 kV 240 MVA auto-transformer have cast doubt on the validity of the algorithm used to estimate moisture content from measured RVM polarisation spectra. A very important influence of oil condition was demonstrated. A limited number of measurements have also been made by NGC with FDS and PDC techniques. Not surprisingly, oil condition is shown to have a significant impact on the responses obtained from these as well.

As a result an alternative interpretation has been proposed, which resolves many previous anomalous moisture determinations. The moisture content in the solid insulation is no longer estimated from the position of the dominant peak in the polarisation spectrum. Instead, the polarisation spectrum is examined for evidence of any subsidiary maxima away from the dominant time constant. The ‘Guuinic’ representation has been found a useful aid in this process, in particular for confirming that the dominant time constant corresponds to the oil peak (narrow ‘nose’) and assessing if there is any sign of polarisation activity above the dominant time constant. Any sub-dominant maximum would likely stem from polarisation

phenomena in the solid insulation. The moisture content is then estimated from this corresponding time constant using the published calibration curves.

In Sweden, ABB and Vattenfall used the three measuring methods on 4 generator step-up transformers (20/400 kV 500 MVA), installed at the Ringhals nuclear power station at the west coast of Sweden, [55]. Two of the transformers have been installed in 1973. They have open conservators and the oil was changed once during their service. Two other transformers have been installed in 1977. They have closed conservators and the oil has never been changed. Distinct differences in the dielectric response spectra were found between the two groups. The results were interpreted and simulated using the methodology presented in section 5; taking into account the materials properties as well as the design of the transformer. With this approach all the three methods ranked the insulation quality equally. Also all three types of measurements were sensitive to the dielectric properties of both the oil and the board and could easily detected small changes in the conductivity of the oil.

Complementary dielectric response measurement on power transformers were also performed in Switzerland and Germany. Results of these activities can be found in [56, 57, 58].

7 CONCLUSIONS AND GUIDELINES

The results of work of TF 15.01.09 presented in this report confirm that the dielectric response measurements provide valuable information on the state of oil-paper insulation in power transformers, in particular the moisture content. All the dielectric response methods compared (RVM, FDS, PDC) reflect the same fundamental polarisation and conduction phenomena in transformer insulation, the special feature of which is a combination of oil gaps and solid insulation.

The dielectric measurements described here confirm that due to the influence of oil gaps, the condition of the oil, specifically its conductivity, has a significant impact on dielectric response, and this must be taken into account when attempting to estimate moisture contents in the solid insulation from the results of all three methods.

Regarding the influence of geometry, it has an influence on the response but not as significant as the effect of the oil conductivity. For the tested sizes of oil gaps, which are typical for the transformer insulation, it is first of all the existence of the gaps rather than their detail dimensions which has the main impact on the results of the measurements.

For the RVM technique, the old interpretation based only on simple relationship between the dominant time constant of the polarisation spectrum and the water content in cellulose is not correct. An improved interpretation requires taking into account the complete measured curve. An alternative qualitative interpretation has been proposed which resolves some previous anomalous conclusions.

Mathematical modelling provides a link between the measured responses of the applied three methods and shows how responses are affected by oil conductivity (resistivity), moisture content and object geometry. Knowledge of the dielectric properties of insulation components is needed for this purpose. Such modelling is recommended today for interpretation of the results of all methods.

Before operational decisions concerning life management of transformers can be made with confidence from the indications of the dielectric response techniques, further validation is required. There is a particular need to verify the estimates of water content determined by the dielectric response techniques by comparison with basic chemical measurements. The influences of different types of pressboard/paper and ageing products (beyond the effects of oil conductivity and moisture) on dielectric response have yet to be determined conclusively.

Since all three methods use different measurements, they could in principle and appear to have in practice, their own strengths and weaknesses. These need to be assessed further before any one can be recommended over the others.

8 REFERENCES

1 Du, Y.; Zahn, M.; Lesieutre, B.C.; Mamishev, A.V.; Lindgren, S.R., **”** Moisture equilibrium in transformer paper-oil systems”, IEEE Electrical Insulation Magazine, Vol. 15, No.1, 1999, pp. 11-20.

2 Kachler A.J., Baehr R., Zaengl W.S, Breitenbauch B., Sundermann U. ”Kritische Anmerkungen zur Feuchtigkeitsbestimmung von Transformatoren mit der "Recovery-Voltage-Methode"”, Elektrizitätswirtschaft, Jg. 95, Heft 19, pp. 1238-1245, 1996.

3 Kachler A.J. “Ageing and Moisture Determination in Power Transformer Insulation Systems. Contradiction of RVM Methodology, Effects of Geometry and Ion Conductivity”, 2nd International Workshop on Transformers, Lodz, Poland, November 24-27, 1999.

4 Tettex Instruments AG: ***Polarisation spectrum analysis for diagnosis of insulation systems***, Information 29, 1992, TI 29-d/e-04. 92.

5 Bognar, A., L. Kalocsai, G. Csepes, E. Nemeth, J. Schmidt: "Diagnostic Tests of High Voltage Oil-paper Insulating Systems (in Particular Transformer Insulation) using DC Dielectrometrics". Proc. Of the 1990 CIGRE Conference, Paris France, paper 15/33-08, 1990.

6 Gäfvert U., Frimpong G., Fuhr J. ”Modelling of Dielectric Measurements on Power Transformers”, Proc. of the 1998 CIGRE Conference, Paris `France, paper 15-103, 1998.

7 Der Houhanessian V. ***Measurement and Analysis of Dielectric Response in Oil-Paper Insulation Systems***, PhD thesis, Swiss Federal Institute of Technology, ETH No. 12832, Zurich, 1998.

8 von Hippel A. R., ”Dielectric Materials and Applications”. The Technology Press of M.I.T. and J. Wiley & Sons, New York, 1958

9 Jonscher A.K., ***Dielectric relaxation in solids***, Chelsea Dielectrics Press, 1983.

10 Debye P., ***Polar Molecules***, The Chemical Catalog Company, New York, 1929.

11 Maxwell J.C. ***A Treatise on Electricity and Magnetism***, vol. 1, Clarendon Press, Oxford, 3rd edition, reprint by Dover, pp. 450-464, 1981.

12 Wagner K.W., ”Erklärung der dielektrischen Nachwirkungsvorgänge auf Grund Maxwellacher Vorstellungen”, Archiv für Elektrotechnik, vol II, no. 9, pp. 371-387, 1914.

13 Sillars R.W. ”The Properties of Dielectric Containing Semiconducting Particles of Various Shapes”, Journal of Institution of Electrical Engineers, vol. 81, pp. 378-394, 1937.

14 Hanai T. ”Theory of Dielectric Dispersion due to Interfacial Polarisation and its Application to Emulsions”, Kolloid Zeitschrift, vol. 171, pp. 23-31, 1960.

15 Steeman P.A.M., Maurer F.H.J. ”Dielectric Monitoring of Water Absorption in Glass-bead-filled High Density Polyethylene”, Colloid & Polymer Science, vol. 286, no. 3, pp. 315-350, 1990.

16 Sihvola A. Lindell I.V. ”Polarizability and Effective Permittivity of Layered and Discontinuously Inhomogeneous Dielectric Elipsoids”, Journal of Electromagnetic Waves and Applications, vol. 4, no. 1, pp. 1-26, 1990.

17 Helgeson A. ***Analysis of Dielectric Response Measurement Methods and Dielectric Properties of Resin-reach Insulation During Processing***, PhD thesis, Royal Institute of Technology (KTH), Stockholm, Sweden, 2000, ISSN 1100-1593.

18 Helgeson A., Gäfvert U. ”Calculation of the Dielectric Response Function from Recovery Voltage Measurements”, Proc. of the 1995 IEEE Conference on Electrical Insulation and Dielectric Phenomena (CEIDP), Virginia Beach USA, pp. 97-101, 1995.

19 Bognar, G. Csepes, L. Kalocsai, I. Kispal: "Spectrum of polarisation phenomena of long time-constant as a diagnostic method of oil-paper insulation systems".Proc. of the 3rd Int. Conf. on Properties and Applications of Dielectric Materials, July 8-12, 1991, Tokyo, Japan, pp.723-726.

20 Bognar, G. Csépes, I. Hamos, I. Kispal and P. Osvath, "Comparing Various Methods for the Dielectric Diagnostics of Oil-Paper Insulation Systems in the range of Low Frequencies or Long Time Constants", 8th Int. Symp. High Voltage Engineering (ISH), Yokohama, Aug. 1993, paper 21.01.

21 Gedde U. ***Polymer Physics***, Chapman & Hall, London UK, 1995.

22 Gäfvert U. ”Condition Assessment of Insulation Systems”, Proc. of the Nordic Insulation Symposium (NORDIS-96), Bergen Norway, pp. 1-20, 1996.

23 Jonscher A.K., Levesque L. ”Volume Low Frequency Dispersion in a Semi-insulating System”, IEEE Trans. On Electrical Insulation, vol. 23, no. 2, pp. 209-213, 1988.

24 Guidi W.W., Fullerton H.P. ”Mathematical Model for Prediction of Moisture Take-up and Removal in Large Power Transformer”, IEEE Winter Power Meeting, New York, Conf. paper C-74 242-4, 1974.

25 Krause C., Gasser H.P., Huser J., Sidler A. ”Effects of Moisture in Transformerboard Insulation and the Mechanism of Oil Impregnation of Voids”. "Transform 98" Conference, Munich, 20. - 21 April 1998 (Forum der Technik).

26 Lampe W. ”Beitrag zur Berechnung der notwendigen Trocknungszeit von Grosstransformatoren”, Archiv für Elektrotechnik, Band 53, Heft 3, 1969.

27 Whitehead J. B., ***Impregnated Paper Insulation***. John Willey & Sons, New York, 1935.

28 Tareev B. ***Physics of Dielectric Materials***. Mir Publishers, 1979.

29 Kind D., Kärner H. ***High Voltage Technology***. Vieweg, 1985.

30 Beyer M., Boeck W., Möller K., Zaengl W. ***Hochspannungstechnik, Theoretische und praktische Grundlagen für die Anwendung,*** Springer, 1986, ISBN 3-540-16014-0.

31 IEC publication 60422 (1998-08). ***Supervision and maintenance guide for insulating mineral oils in electrical equipment.***

32 Sillars W., ***Electrical Insulating Materials and their Application.*** Billing&Sons, London, 1973.

33 Farooq K. “The Effect of Particulate and Water Contamination on the Dielectric Strength of Insulating Oils”, Conference record of the 1996 IEEE International Symposium on Electrical Insulation, vol. 2, pp. 728-732, 1996.

34 Itahashi S., Mitsui H., Sato T., Sone M. ”State of Water in Hydrocarbon Liquids and its Effect on Conductivity”, IEEE Transaction on Dielectrics and Electrical Insulation, Vol. 2, No. 6, pp. 1117-1122, 1995.

35 Washabaugh A.P., Mamishev A., Du Y., Zahn M.: ”Dielectric Measurements of Semi-insulating Liquids and Solids”**,** Conference Record of ICDL'96, 12th International Conference on Conduction and Breakdown in Dielectric Liquids, Rome, IEEE Publication 96CH35981, pp. 381-384, 1996.

36 Harrison N.L, ”Resistivity of Transformer Oil at Low and Medium Field Strengths”, Proc. Inst. Electr. Eng., Vol.115, pp. 736-741, 1968.

37 Diabi R., Filippini J.C., Marteau C., Tobazéon R. ”On the role of temperature and impurities in the low field conduction of insulating liquids”, Conference Record of ICDL'96 12th International Conference on Conduction and Breakdown in Dielectric Liquids, Rome, IEEE Publication 96CH35981, pp. 350-353, 1996.

38 Denat A. ***Etude de la Conduction Electrique dans les Solvants Non Polaires***, Thesis L'Universit Scientifique et Mdicale et L'Institute National Polytechnique de Grenoble, 1982.

39 Gäfvert U., Jaksts A., Törnkvist C., Wahlfridsson L. "Electrical Field Distribution in Transformer Oil", IEEE Trans on Electrical Insulation, Vol. 27 No.3, 1992, p.647.

40 Gäfvert U., Kols H. "Simple method for Determining the Electrical Conductivity in Transformer oil", Conf. Record of Nordic Insulation Symposium, Helsinki, Finland, June 9-11, 1986, p.23:1.

41 Der Houhanessian V. ***Measurement and Analysis of Dielectric Response in Oil-Paper Insulation Systems***, PhD thesis, Swiss Federal Institute of Technology, ETH No. 12832, Zurich, 1998.

42 Tobazéon R., Filippini J.C., Marteau C. ”On the Measurement of the Conductivity of Highly Insulating Liquids”, IEEE Transactions on Dielectrics and Electrical Insulation, Vol. 1 No. 6, pp. 1000-1004, 1994.

43 Gäfvert U., Kols H., Marinko J. ”Simple Method for Determining the Electric Conductivity of Dielectric Liquids”, Nordic Insulation Symposium, Helsinki Finland, paper 23, pp. 1-5, 1986.

44 Li Y., Rungis J. ”The Square Wave Voltage Method for the Measurement of Low Level tanδ of Liquid Dielectrics”, 1997 IEEE International Conference on Properties and Applications of Dielectric Materials, IEEE Publication 97CH35794, pp. 1125-1128, 1997.

45 von Münch W. ***Elektrische und magnetische Eigenschaften der Materie,*** B. G. Teubner Stuttgart, 1987.

46 Bartnikas R. ***Engineering Dielectrics - Volume III - Electrical Insulating Liquids,*** ASTM, Philadelphia, 1994, ISBN 0-8031-2055-9.

47 Ekanayake C. ***Application of Dielectric Spectroscopy for Estimating Moisture Content in Power Transformers***, Lic. thesis, Chalmers University of Technology (CTH), Gothenburg, Sweden, 2003, Techn. Rep. No. 465L.

48 Jonscher A:K., Ramdeen A. "Transient Dielectric Response of Conduction on Humid Mica", IEEE Trans. on Electrical Insulation, vol. 22, pp. 35-39, 1987.

49 Neimanis R. ***On estimation of Moisture Content in Mass Impregnated Distribution Cables,*** PhD thesis, Royal Institute of Technology (KTH), Stockholm, Sweden, 2001, ISSN 1100-1593.

50 Tettex Instruments AG: ***Polarisation spectrum analysis for diagnosis of insulation systems***, Information 29, 1992, TI 29-d/e-04. 92.

51 Gäfvert U., Frimpong G., Fuhr J. "Modelling of Dielectric Measurements on Power Transformers", Proc. of the 1998 CIGRE Conference, Paris `France, paper 15-103, 1998.

52 Gäfvert U., Ildstad E. "Modelling Return Voltage Measurements of Multi-layer Insulation Systems", Proc. of the 4th Intern. Conf. On Properties and Application of Dielectric Materials, Brisbane Australia, pp. 123-126, 1994.

53 Der Houhanessian V., Zaengl W.S. "On-site diagnosis of power transformers by means of relaxation current measurements", Conference Record of the 1998 IEEE International Symposium on Electrical Insulation, IEEE Publication 98CH36239, pp. 28-34.

54 Lapworth J., Heywood R. "The Determination of the Dryness of Transformer Insulation: Recent NGC Experience with Polarisation Tests", Proc. Of the Transformer 01 Conference, Bydgoszcz Poland, pp. 84-94, 2001.

55 Gäfvert U, Adeen L., Tapper M., Ghasemi P., Jönsson B. "Dielectric Spectroscopy in Time and Frequency Domain Applied to Diagnostics of Power Transformers", Proc. Of the 6th Intern. Conf. On Properties and Applications of Dielectric Materials (ICPADM), Xian China, pp. 825-830, 2000.

56 Aschwanden T., Hässig M., Fuhr J., Lorin P., Der Houhanessian V., Zaengl W., Schenk A., Zweiacker P., Piras A., Dutoit J. "Development and application of new condition assessment methods for power transformers", CIGRE 1998 Session, paper 12-207.

57 Hässig M., Bräunlich R., Gysi R., Alff J.-J., Der Houhanessian V., Zaengl W.S. "On-Site Application of Advanced Diagnosis Methods for Quality Assessment of Insulation of Power Transformers", Annual Report of the 2001 Conference on Electrical Insulation and Dielectric Phenomena, IEEE Publication 01CH37225, pp. 441-447.

58 Leibfried T., Kachler A.J., Zaengl W.S., Der Houhanessian V., Küchler A., Breitenbauch B. "Ageing and Moisture Analysis of Power Transformer Insulation Systems", CIGRE 2002 Session, paper 12-101.